UPPSALA UNIVERSITET

Division of Materials Theory
DMT
Uppsala Universitet

# Density Functional Theory Applied To Magnetism

Biplab Sanyal
Department of Physics & Astronomy,
Uppsala University, Sweden

**3rd July, 2025**
**European School of Magnetism**
**Liege, Belgium**

Vetenskapsrådet

STINT
Stiftelsen för internationalisering av högre utbildning och forskning

CSC SCHOLARSHIP
A WAY TO YOUR DREAMS

SNIC
NAISS

EuroHPC
Joint Undertaking

# European School on Magnetism 2026

# Spin-orbit driven magnetic phenomena

**Ångström laboratory, Uppsala University, Sweden**

**August 17-28, 2026**

Enjoy ten days of fascinating topics around magnetism at the oldest university of Scandinavia. Lectures and hands-on sessions will cover fundamental aspects, theoretical modelling as well as experimental characterization of a variety of topics:

- Nanomagnetism
- Ultrafast magnetization dynamics
- Spin-orbit torques
- Spin-dependent transport
- Spin and orbital Hall effect
- Skyrmions
- Permanent magnets
- 2D magnets
- AFM spintronics
- Altermagnetism…

Organization:
ESM chair: Assoc. Prof. Biplab Sanyal
ESM co-chair: Dr. Heike Herper

UPPSALA UNIVERSITET

# Plan for today

- Short introduction to (s)DFT
- Spin dipole moments
- Electron correlation (DFT+U & DMFT)
- Magnetic exchange interactions
- Magnetic anisotropy
- 2D magnets
- Atomistic spin dynamics simulations

# Bridging length and time scales

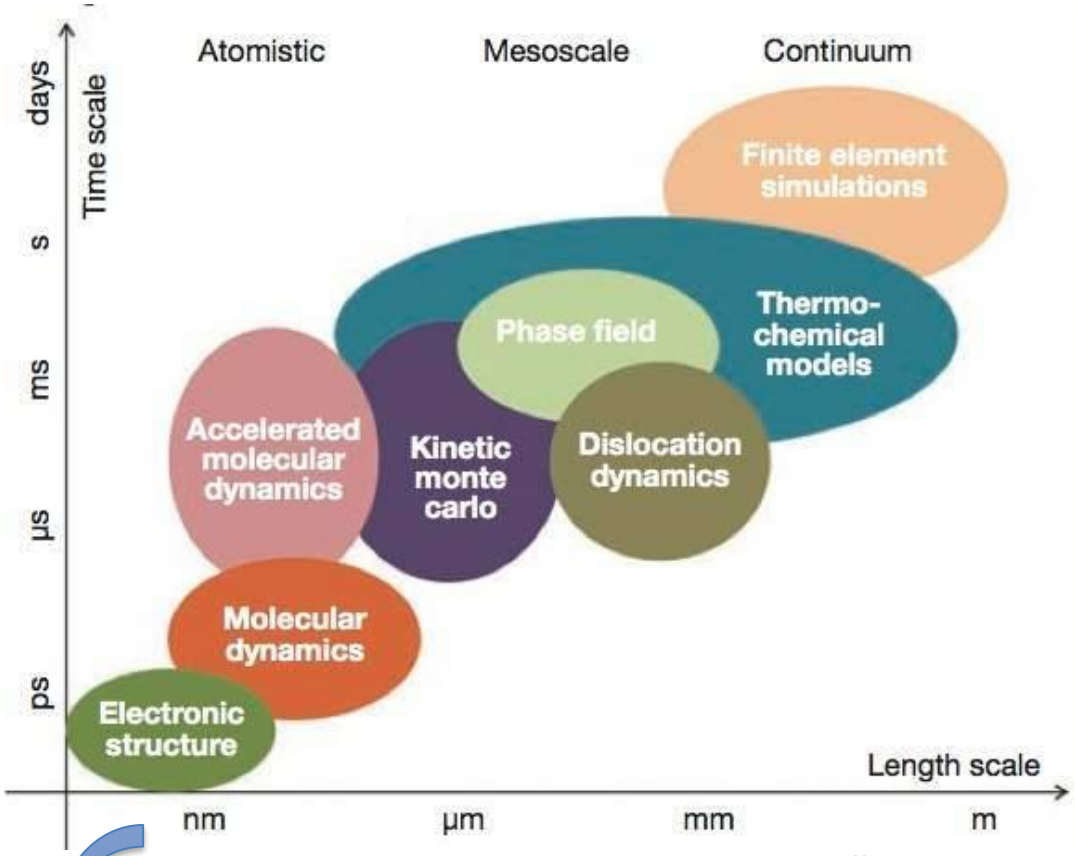


## Multiscale magnetism

DFT

↓

Atomistic spin-lattice model

↓

Monte Carlo simulation
Atomistic spin dynamics
Micromagnetics

J. Alloy. Comp. **444**, 415 (2007)

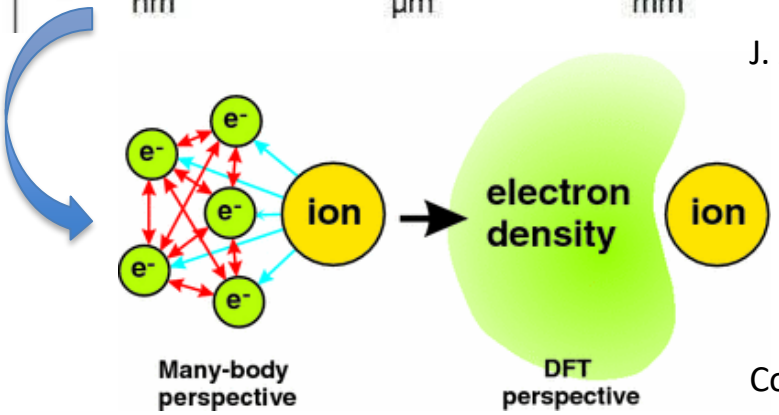


Courtesy: Springer

# Hamiltonian for a many particle system reads

$$H = -\frac{1}{2}\sum_{i=1}^{N}\nabla_i^2 - \frac{1}{2}\sum_{A}^{M}\frac{1}{M_A}\nabla_A^2 - \sum_{i=1}^{N}\sum_{A=1}^{M}\frac{Z_A}{|\mathbf{r}_{iA}|} + \sum_{i=1}^{N}\sum_{j>i}^{N}\frac{1}{|\mathbf{r}_{ij}|} + \sum_{A=1}^{M}\sum_{B>A}^{M}\frac{Z_A Z_B}{|\mathbf{R}_{AB}|}$$

K.E. of electrons

K.E. of nuclei

Electron-nucleus attraction

Electron-electron repulsion

nucleus-nucleus repulsion

Born-Oppenheimer approximation → **Decouple electronic and nuclear degrees of freedom**

## Hamiltonian for electron system only

$$H_{elec} = -\frac{1}{2}\sum_{i=1}^{N}\nabla_i^2 - \sum_{i=1}^{N}\sum_{A=1}^{M}\frac{Z_A}{|\mathbf{r}_{iA}|} + \sum_{i}^{N}\sum_{j>i}^{N}\frac{1}{|\mathbf{r}_{ij}|}$$

Schroedinger equation for electron system only

$$H_{el}\phi_{el} = E_{el}\phi_{el}$$

The electronic wave function reads

$$\phi_{el} = \phi_{el}(\{\mathbf{r}_i\};\{\mathbf{R}_A\})$$

# Density functional theory

Hohenberg-Kohn energy functional

$$E_{HK}[n] = T[n] + E_{\text{int}}[n] + \int dr V_{ext}(r) n(r) + E_{II}$$

**Kohn Sham ansatz:**

Replace the interacting many body system by a non-interacting auxiliary system with the same ground state density

$$E_{KS} = T_S[n] + \int dr V_{ext}(r) n(r) + E_H[n] + E_{II} + E_{XC}[n]$$

$$T_S = \frac{1}{2} \sum_s \sum_{i=1}^{N_s} \left| \nabla y_i^s \right|^2$$

$$E_H = \frac{1}{2} \int dr\, dr' \frac{n(r) n(r')}{\left| r - r' \right|}$$

$$E_{XC}[n] = \left\langle T \right\rangle - T_S[n] + \left\langle V_{\text{int}} \right\rangle - E_H[n]$$

# Generalized spin density functional theory

Bluegel, IFF Spring School ('14)

Kohn-Sham equation

$$[-\frac{\hbar^2}{2m}\nabla^2 + v(\mathbf{r}) + \int \frac{n(\mathbf{r}')}{|\mathbf{r}-\mathbf{r}'|}d\mathbf{r}' + \frac{\delta E_{XC}}{\delta n(\mathbf{r})}]\phi_i(\mathbf{r}) = \epsilon_i\phi_i(\mathbf{r})$$

Electron density $n(\mathbf{r}) = \sum_{i=1}^{N} |\phi_i(\mathbf{r})|^2$

Generalization to spin DFT (Barth & Hedin (1972))

2x2 spin-density matrix $n_{\alpha\beta}(\mathbf{r}) = \sum_{i=1}^{N} \phi_i^{*\alpha}(\mathbf{r})\phi_i^{\beta}(\mathbf{r})$

$$\underline{\mathrm{n}}(\mathbf{r}) = \frac{1}{2}(n(\mathbf{r})\mathrm{I} + \sigma \cdot \mathbf{m}(\mathbf{r}))$$

$$= \frac{1}{2}\begin{pmatrix} n(\mathbf{r}) + m_z(\mathbf{r}) & m_x(\mathbf{r}) - im_y(\mathbf{r}) \\ m_x(\mathbf{r}) + im_y(\mathbf{r}) & n(\mathbf{r}) - m_z(\mathbf{r}) \end{pmatrix}$$

# Spin density functional theory (contd.)

Similarly, potential matrices are written as

$$\underline{\mathrm{v}}(\mathbf{r}) = v(\mathbf{r})\mathrm{I} + \mu_B \sigma \cdot \mathbf{B}(\mathbf{r})$$

$$\underline{\mathrm{v}}_{\mathrm{XC}}(\mathbf{r}) = v_{\mathrm{XC}}(\mathbf{r})\mathrm{I} + \mu_B \sigma \cdot \mathbf{B}_{\mathrm{XC}}(\mathbf{r})$$

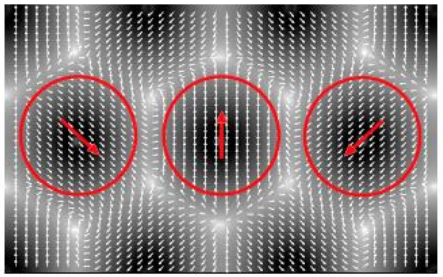

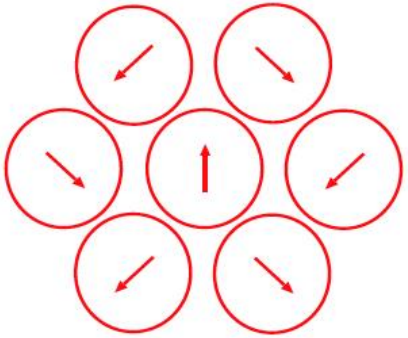

Magnetic ground state of hexagonal Cr monolayer

For collinear case

$$(\frac{\hbar^2}{2m}\nabla^2 + v_{Coul}(\mathbf{r}) + B_z(\mathbf{r}) + v^{\uparrow}_{XC}(\mathbf{r}))\phi^{\uparrow}_i(\mathbf{r}) = \epsilon^{\uparrow}_i \phi^{\uparrow}_i(\mathbf{r})$$

$$(\frac{\hbar^2}{2m}\nabla^2 + v_{Coul}(\mathbf{r}) - B_z(\mathbf{r}) + v^{\downarrow}_{XC}(\mathbf{r}))\phi^{\downarrow}_i(\mathbf{r}) = \epsilon^{\downarrow}_i \phi^{\downarrow}_i(\mathbf{r})$$

# Performance of DFT

## Comparison between theory and experiment

Magnetic moments ($\mu_B$)

| Property | source | Fe (bcc) | Co (fcc) | Ni (fcc) | Gd (hcp) |
|---|---|---|---|---|---|
| $M_{spin}$ | LSDA | 2.15 | 1.56 | 0.59 | 7.63 |
| $M_{spin}$ | GGA | 2.22 | 1.62 | 0.62 | 7.65 |
| $M_{spin}$ | experiment | 2.12 | 1.57 | 0.55 | |
| $M_{tot.}$ | experiment | 2.22 | 1.71 | 0.61 | 7.63 |

Exchange-correlation

LSDA:
Local spin density approximation

GGA:
Generalized gradient approximation

Binary random alloys

Slater-Pauling curve (an interesting trend)

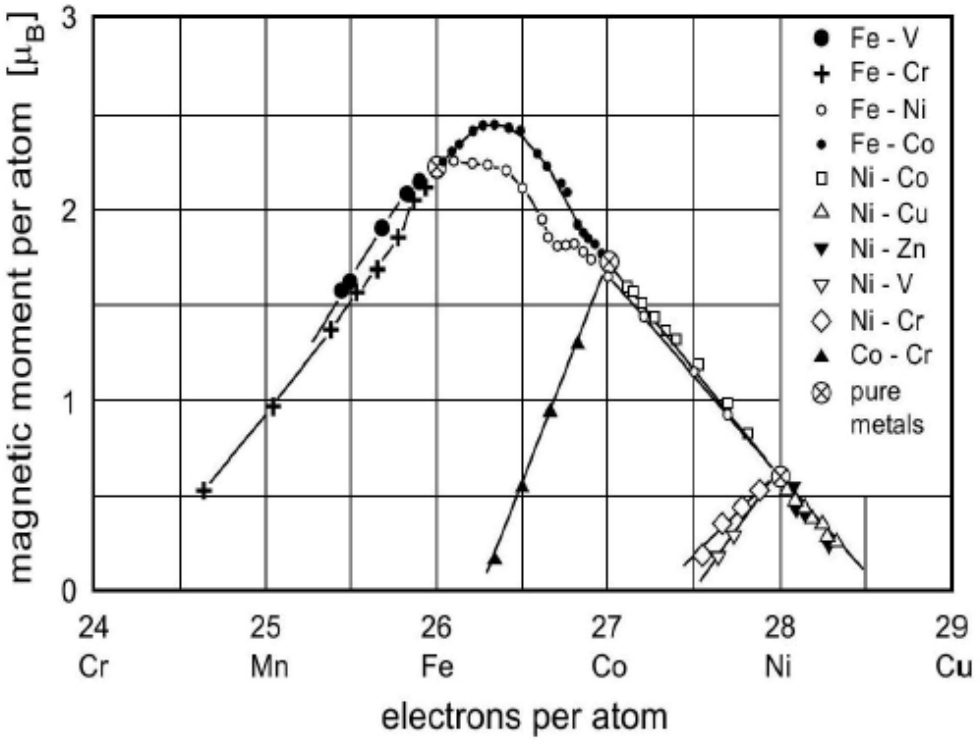

# Binary random alloys

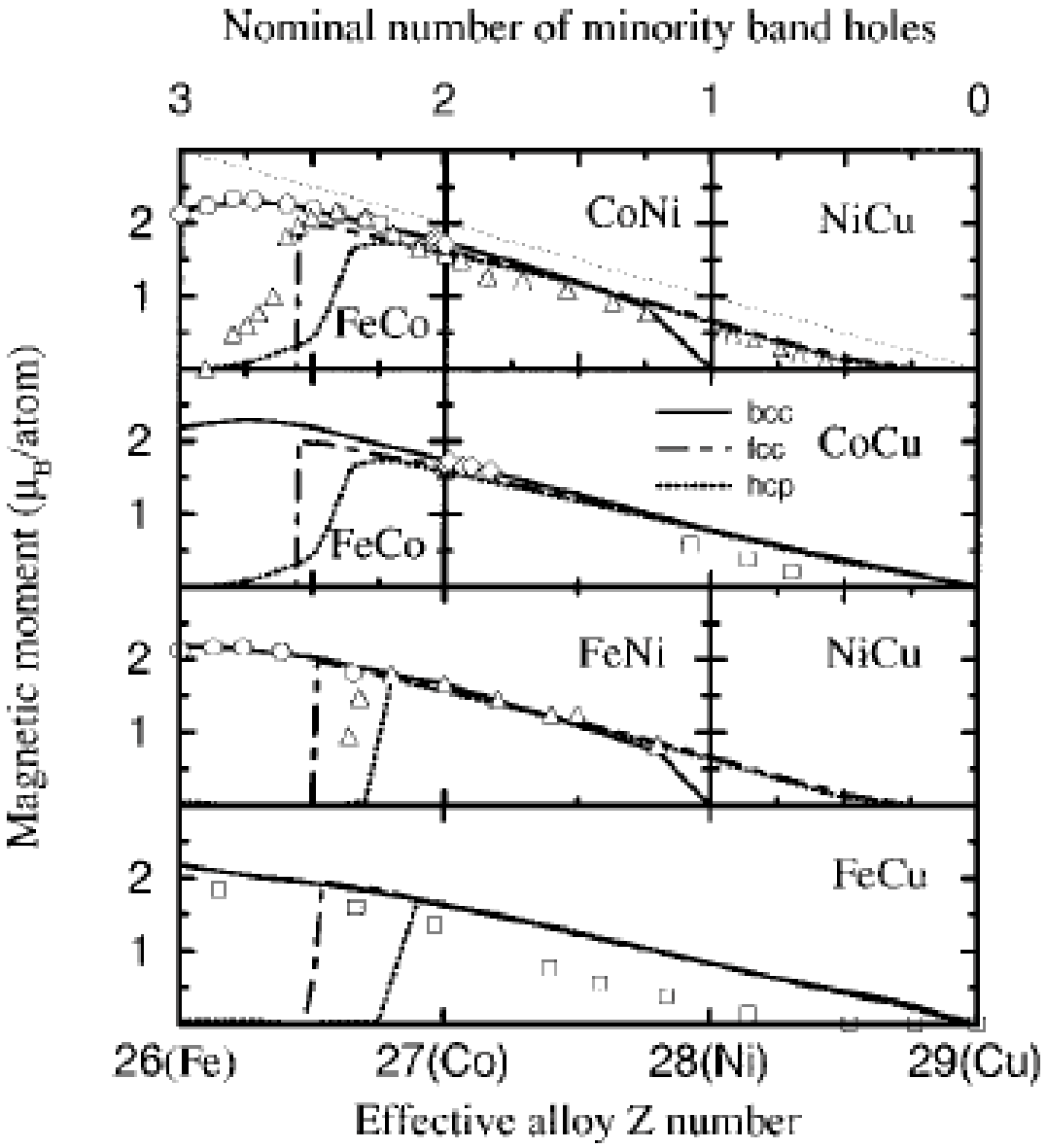


LMTO +
Coherent Potential
Approximation (CPA)

PRB **59**, 419 (1999)

# Element-specific magnetic measurements

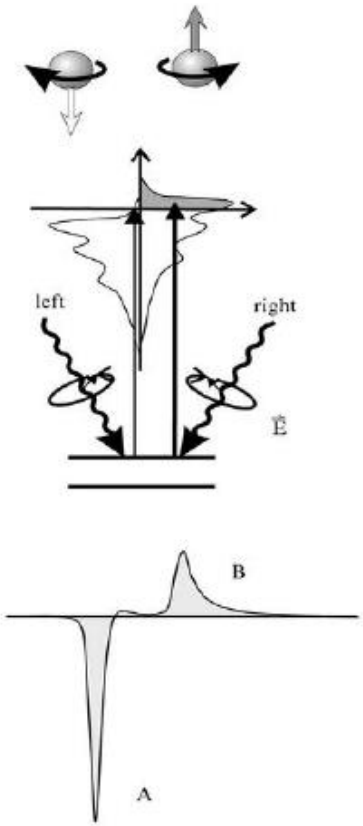


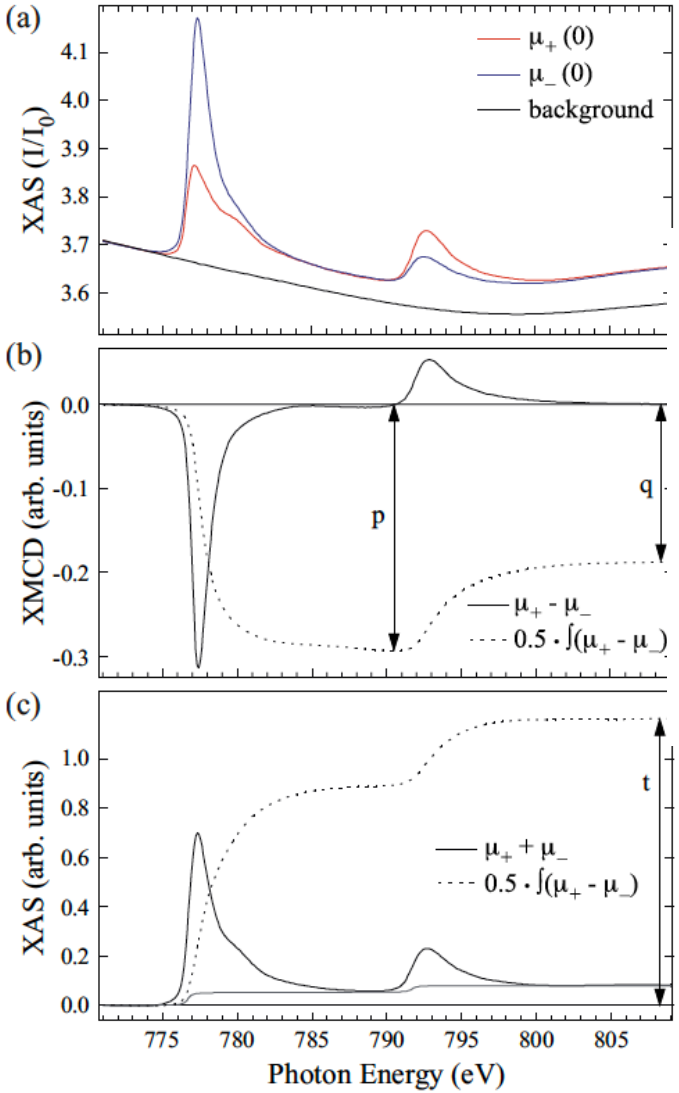


Sum rules

spin and orbital moments

$$L = -\frac{4}{3}h_d \frac{\int_{L_3+L_2}(\mu_+ - \mu_-)dE}{\int_{L_3+L_2}(\mu_+ + \mu_-)dE} = -\frac{4}{3}h_d\frac{q}{t}, \qquad (1)$$

$$S + 7D = -h_d \frac{6\int_{L_3}(\mu_+ - \mu_-)dE - 4\int_{L_3+L_2}(\mu_+ - \mu_-)dE}{\int_{L_3+L_2}(\mu_+ + \mu_-)dE}$$

$$= -h_d\frac{6p-4q}{t}, \qquad (2)$$

XAS: X-ray absorption spectroscopy

XMCD: X-ray magnetic circular dichroism

# Spin-dipolar contribution

XMCD: $m_{eff}=m_S+7\langle T_z\rangle$

Angular dependence

$$m_{eff}(q)=m_S+7T(q)$$
$$T(q)\sim\frac{1}{2}(3Cos^2q-1)$$

PRB **82**, 014405 (2010)

Spin dipole operator:

$$T=\sum_i\left[s^{(i)}-3\frac{r^{(i)}(r^{(i)}\cdot s^{(i)})}{\left|r^{(i)}\right|^2}\right]$$

$$T=\sum_i Q^{(i)}s^{(i)}$$

Quadrupolar tensor $Q^{(i)}_{ab}=d_{ab}-3\hat{r}^{(i)}_a\hat{r}^{(i)}_b$

$$T_\pm=\sum_{nn\sigma}T^{(\pm)}_{nn\sigma}a^+_n a_{n\sigma}$$

$$T_z=\sum_{nn\sigma}T^{(z)}_{nn\sigma}a^+_n a_{n\sigma}$$

$$c^{(l)}_m(\hat{r})=\sqrt{\frac{4p}{2l+1}}Y_{lm}(\hat{r})$$

$$T^{(\pm)}_{\nu\nu'}=\left\langle\nu\left|c^{(2)}_0 s_\pm-\sqrt{6}c^{(2)}_{\pm2}s_\mp\pm\sqrt{6}c^{(2)}_{\pm1}s_z\right|\nu'\right\rangle \qquad |n\rangle=|l,m,s\rangle$$

$$T^{(z)}_{nn\sigma}=\left\langle n\left|-\sqrt{\frac{3}{2}}c^{(2)}_1 s_+ +\sqrt{\frac{3}{2}}c^{(2)}_1 s_- -2c^{(2)}_0 s_z\right|n\sigma\right\rangle$$

Crystal field

No spin-flip

Oguchi and Shishidou, Phys. Rev. B **70**, 024412 (2004).

# Importance of spin-dipolar contribution

Verwey transition (cubic -> monoclinic)

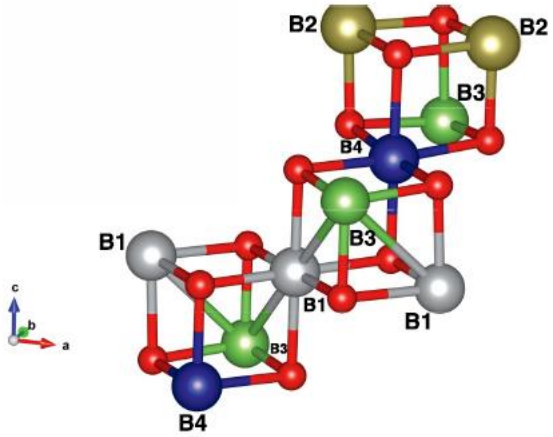


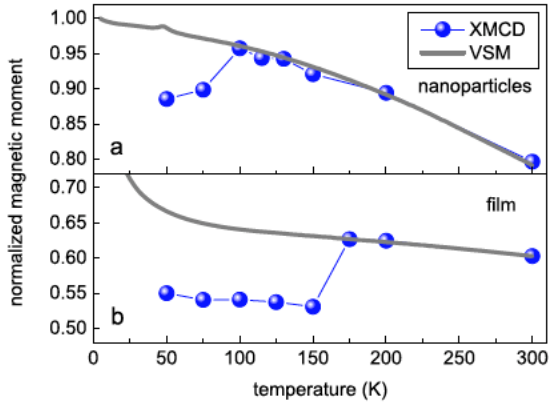


Table I | Charge, spin and magnetic dipole moments for 3d orbitals of Fe atoms at different sites in the monoclinic unit cell. Also, effective moments ($\mu_{S,eff} = -2\langle S_z\rangle \mu_B + 7\langle T_z\rangle \mu_B$) are provided. The Fe sites are named as in Ref. [17]

| Fe site | d-charge | $-2\langle S_z\rangle$ | $7\langle T_z\rangle$ | $\mu_{S,eff}$ ($\mu_B$) |
|---|---|---|---|---|
| A1 | 5.91 | −3.98 | −0.015 | −3.995 |
| A2 | 5.91 | −3.98 | 0.025 | −3.955 |
| B1 | 6.08 | 3.67 | 0.72 | 4.39 |
| B2 | 5.82 | 4.14 | 0.043 | 4.183 |
| B3 | 5.85 | 4.08 | 0.027 | 4.107 |
| B4 | 6.1 | 3.64 | −1.44 | 2.20 |

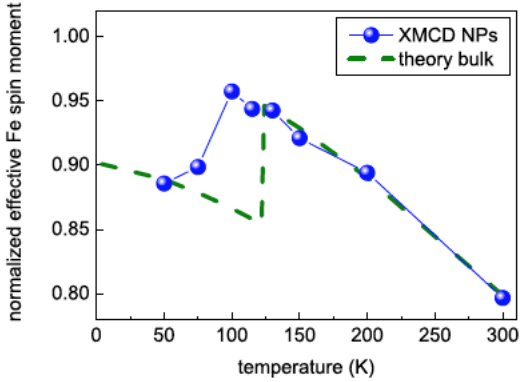


Sci. Rep. **4**, 5760 (2014)

# Strong electron correlation

## Transition metal oxides

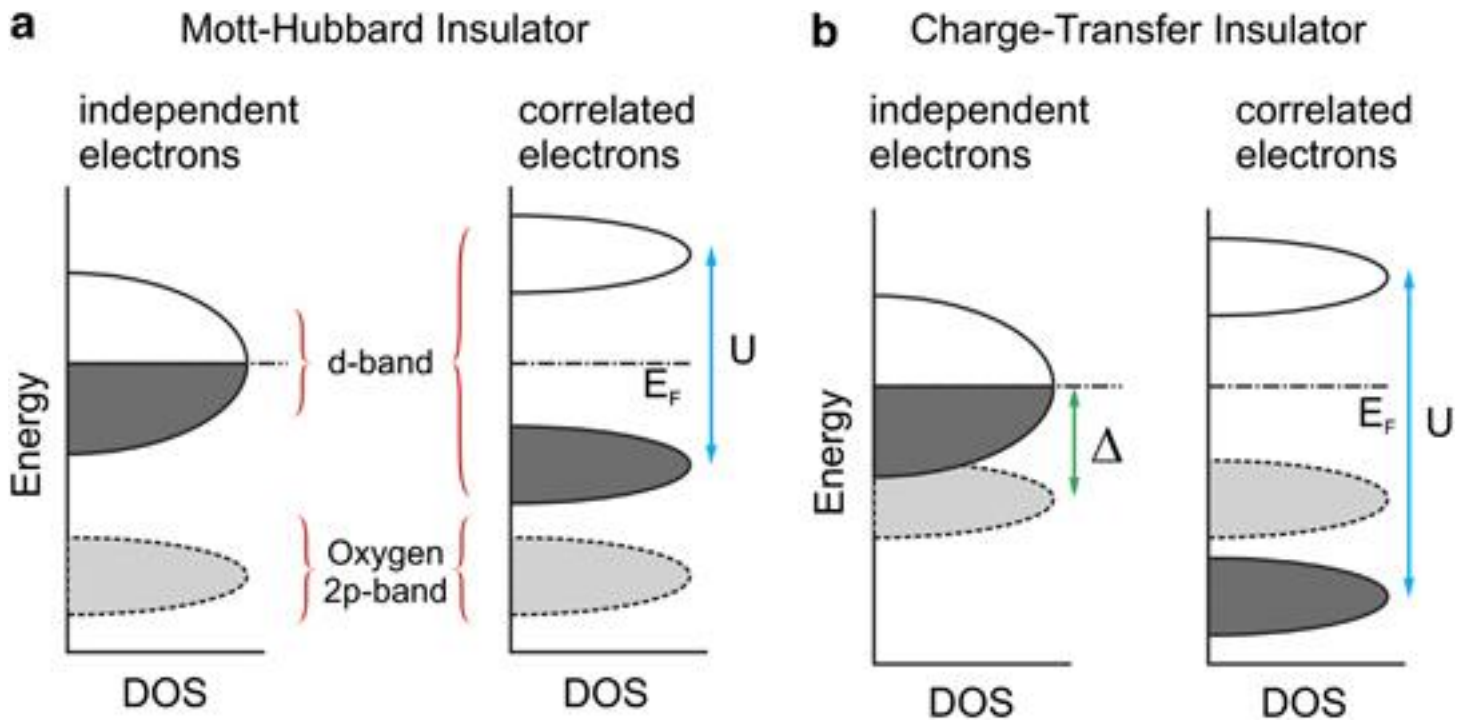


V-O, Ti-O

Ni-O, Cu-O

# DFT+U (Hubbard formalism)

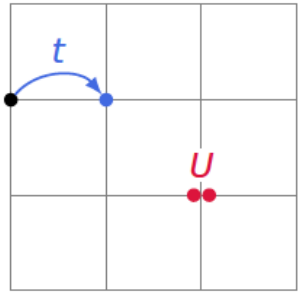


Hubbard Hamiltonian

$$H = -t \sum_{<i,j>,\sigma} (c^{\dagger}_{i,\sigma} c_{j,\sigma} + c^{\dagger}_{j,\sigma} c_{i,\sigma}) + U \sum_{i=1}^{N} n_{i\uparrow} n_{i\downarrow}$$

Energy functional

$$E = E^{LDA} - U\frac{N(N-1)}{2} + \frac{1}{2}U \sum_{p \neq q} n_p n_q$$

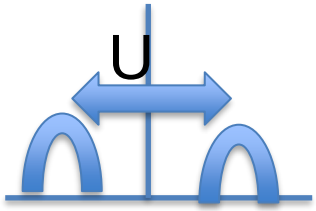


Orbital energy

$$\epsilon_p = \frac{\partial E}{\partial n_p} = \epsilon^{LDA} + U(\frac{1}{2} - n_p)$$

$n_p$=1 → $\varepsilon_p = \varepsilon_{LDA}$-U/2

$n_p$=0 → $\varepsilon_p = \varepsilon_{LDA}$+U/2

# LDA+U (contd.)

Generalized LDA+U functional

$$E^{LDA+U}[\rho^\sigma(\mathbf{r}),\{n^\sigma\}] = E^{LSDA}[\rho^\sigma(\mathbf{r})] + E^U[\{n^\sigma\}] - E_{dc}[\{n^\sigma\}]$$

Matrix elements of screened Coulomb interactions

$$\langle m,m''|V_{ee}|m',m'''\rangle = \sum_k a_k(m,m',m'',m''')F^k$$

$0 \le k \le 2l$

$F^k$: Slater integrals

$$a_k(m,m',m'',m''') = \frac{4\pi}{2k+1}\sum_{q=-k}^{k}\langle lm|Y_{kq}|lm'\rangle\langle lm''|Y^*_{kq}|lm'''\rangle$$

$$U = F^0, J = (F^2+F^4)/14$$

$F^2/F^4 \sim 0.625$ for 3d electrons

$J = (286F^2 + 195F^4 + 250F^6)/6435$ for f electrons

# DFT+Hubbard U (electronic structure)

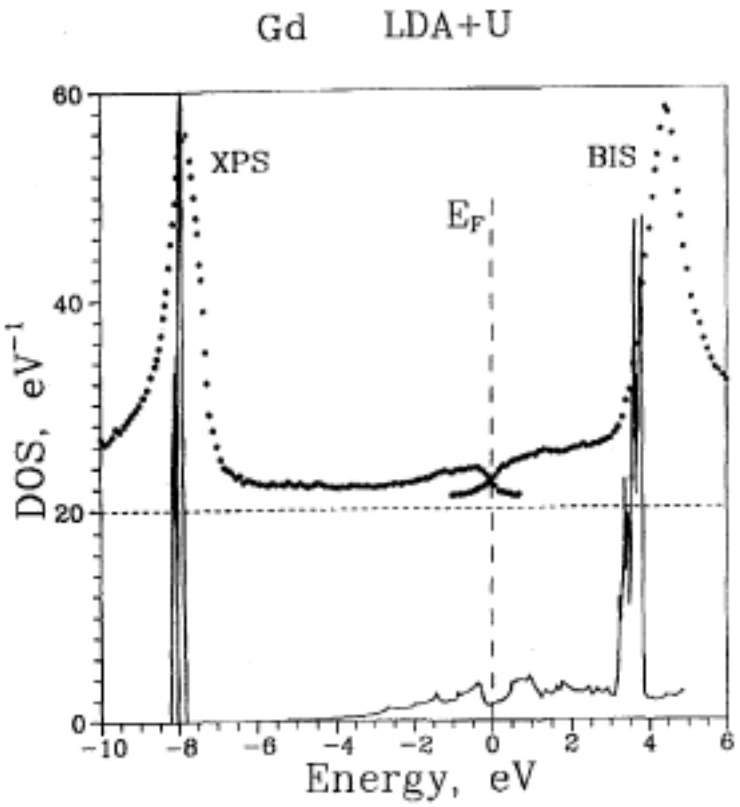


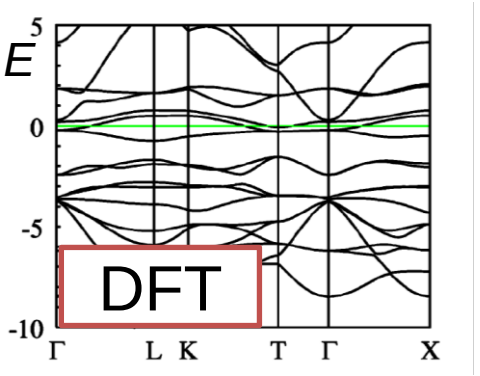


metal

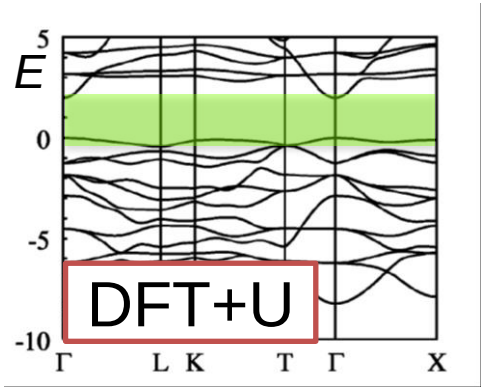


insulator

**Figure 1.** The density of states for ferromagnetic Gd metal from LDA+$U$ calculation and results of BIS (bremsstrahlung isochromat spectroscopy) and XPS (x-ray photoemission spectroscopy) experiments.

V.I. Anisimov, J. Zaanen and O.K. Andersen. *Phys. Rev. B*, (1991).
M. Cococcioni and S. de Gironcoli. *Phys. Rev. B,* (2005).

# Comparison: DFT, DFT+U & Experiments

TABLE II. Experimental (expt) and calculated (LDA + $U$) spin moments ($m$, in $\mu_B$) and energy gaps ($E$, in eV) of the late-3$d$-transition-metal monoxides. For comparison, we also show these quantities as calculated from LSDA (Ref. 1).

| | $E_{\mathrm{LSD}}$ | $E_{\mathrm{LSD}+U}$ | $E_{\mathrm{expt}}$ | $m_{\mathrm{LSD}}$ | $m_{\mathrm{LSD}+U}$ | $m_{\mathrm{expt}}$ |
|---|---|---|---|---|---|---|
| $CaCuO_2$ | 0.0 | 2.1 | 1.5[a] | 0.0 | 0.66 | 0.51[b] |
| CuO | 0.0 | 1.9 | 1.4[c] | 0.0 | 0.74 | 0.65[d] |
| NiO | 0.2 | 3.1 | 4.3,[e]4.0[f] | 1.0 | 1.59 | 1.77,[9]1.64,[h]1.90[i] |
| CoO | 0.0 | 3.2 | 2.4[j,k] | 2.3 | 2.63 (3.60) | 3.35,[l]3.8[m] |
| FeO | 0.0 | 3.2 | 2.4[n] | 3.4 | 3.62 (4.59) | 3.32[m] |
| MnO | 0.8 | 3.5 | 3.6–3.8[o] | 4.4 | 4.61 | 4.79,[g]4.58[i] |

# Magnetic organometallics

Iron porphyrin (FeP)

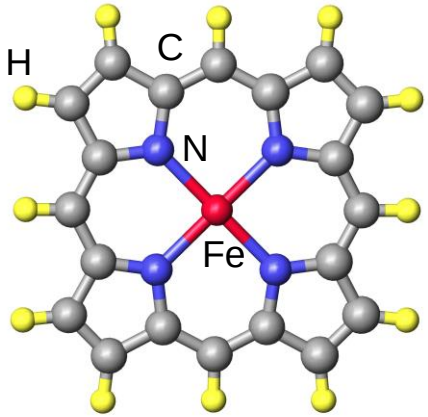


$Fe^{3+}$ ($d^5$)
S=1/2, 3/2, 5/2

$Fe^{2+}$ ($d^6$)
S=0, 1, 2

Iron phthalocyanine (FePc)

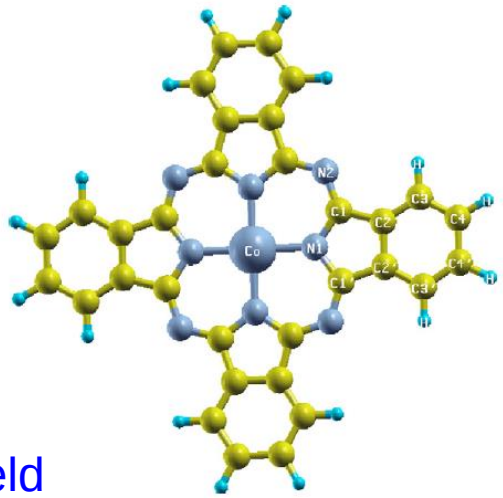

- Spin crossover molecule:
Light, temperature, electric field

Crystal field splitting

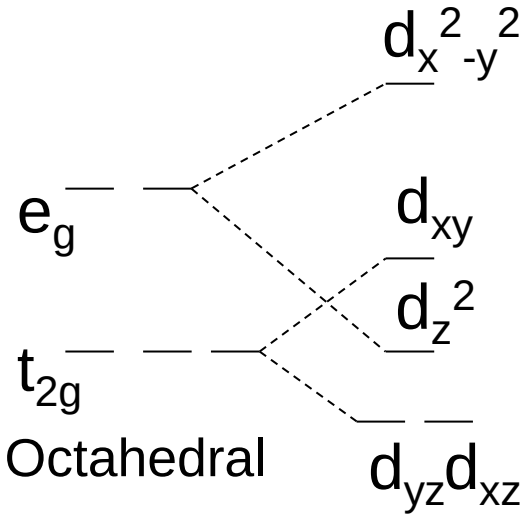


FeP, LDA+U=4 eV, J= 1 eV

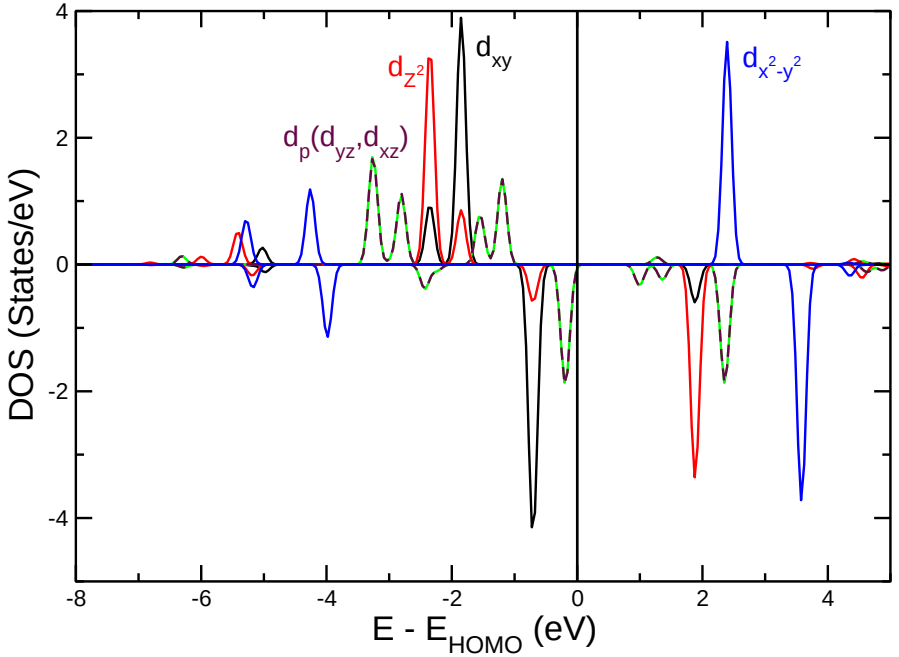

# A meaningful estimation of Hubbard U in DFT+U

B3LYP & HSE06: Hybrid functionals

Effective U ($U_{eff}$) =U-J

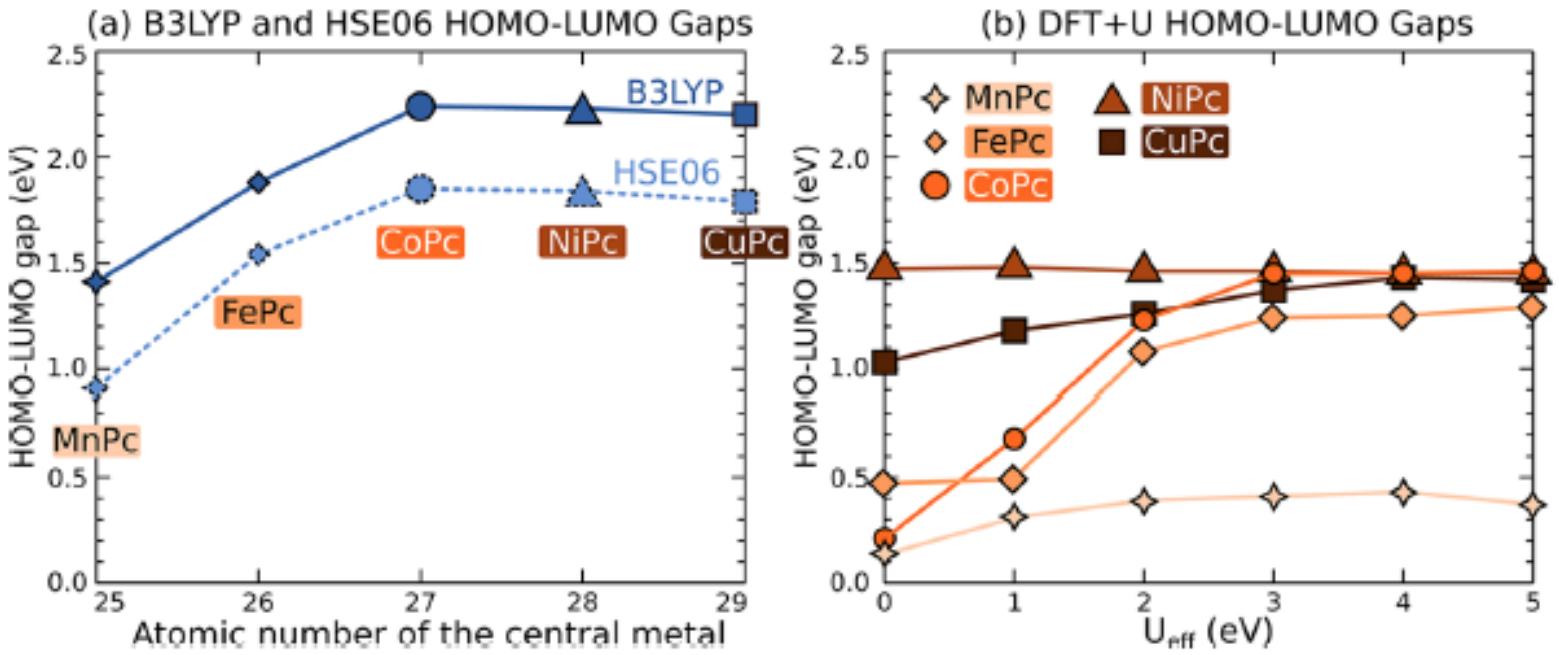


Metal moments ($\mu_B$)

| Molecule | DFT+U | B3LYP | HSE06 |
|---|---|---|---|
| MnPc | 3.42($U_{eff}$=3)<br>3.54($U_{eff}$=4) | 3.43 | 3.57 |
| FePc | 2.03 ($U_{eff}$=5) | 2.10 | 2.12 |
| CoPc | 1.06 ($U_{eff}$=5) | 1.09 | 1.1 |
| NiPc | 0 | 0 | 0 |
| CuPc | 0.57 ($U_{eff}$=2)<br>0.59 ($U_{eff}$=3) | 0.57 | 0.59 |

# Calculation of U from linear response

$$E_{Hub} - E_{dc} = \sum_{I,\sigma} \frac{U_{eff}}{2} Tr[n^{I\sigma}(1 - n^{I\sigma})]$$

$$U = \frac{d^2(E^{DFT})}{d(n^I)^2}$$

$$U = \chi_0^{-1} - \chi^{-1}$$

Difference in response matrices due to perturbation in occupation

## Calculated values of U (eV)

| molecule | $U_0$ (eV) | $U_0^{scf}$ (eV) | $U^{all}$ (eV) | $U_{eff}^{PES}$ (eV) | $\lvert U_0 - U^{all} \rvert$ (eV) |
|---|---|---|---|---|---|
| MnPc | 6.2 | 6.3 | 6.1 | 4 | 0.1 |
| FePc | 4.4 | 4.4 | 4.4 | 4–5 | 0.0 |
| CoPc | 6.1 | 6.1 | 6.0 | 4–6 | 0.1 |
| NiPc | 8.2 | 8.2 | 8.4 | 5–7 | 0.2 |
| CuPc | 3.7 | 3.6 | 4.0 | 4–5 | 0.3 |

MnPc, FePc & CoPc: calculated U values produce good agreement with experimental spectroscopy

Brumboiu et al, J. Chem. Th. Comp. **12**, 1772 (2016)

# Regimes of electron correlation

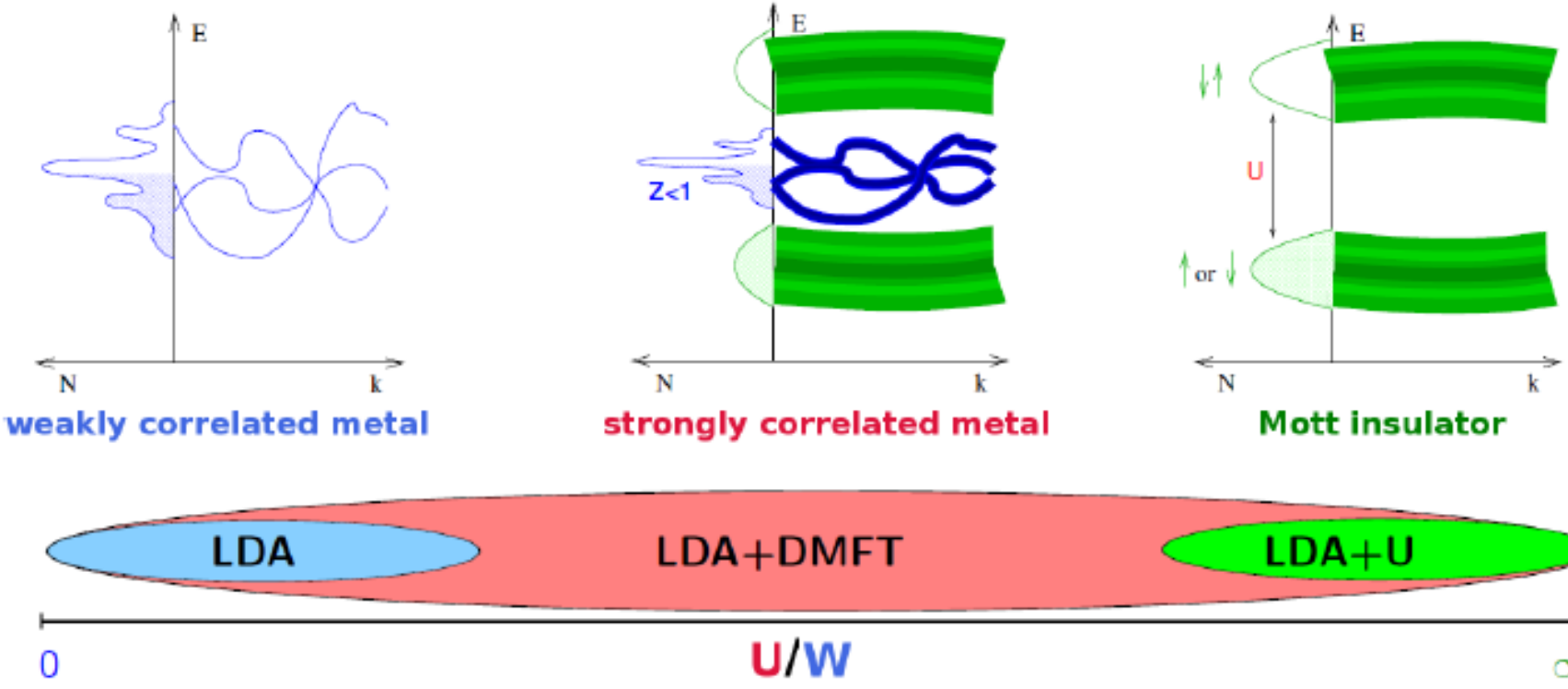


*U*: screened local interaction  *W*: bandwidth, ~ *t*

DFT+U: Static mean field theory
DMFT: Dynamical mean field theory

K. Held, Advances in Physics, 56, 829 (2007)

# DMFT: Lattice to Impurity model

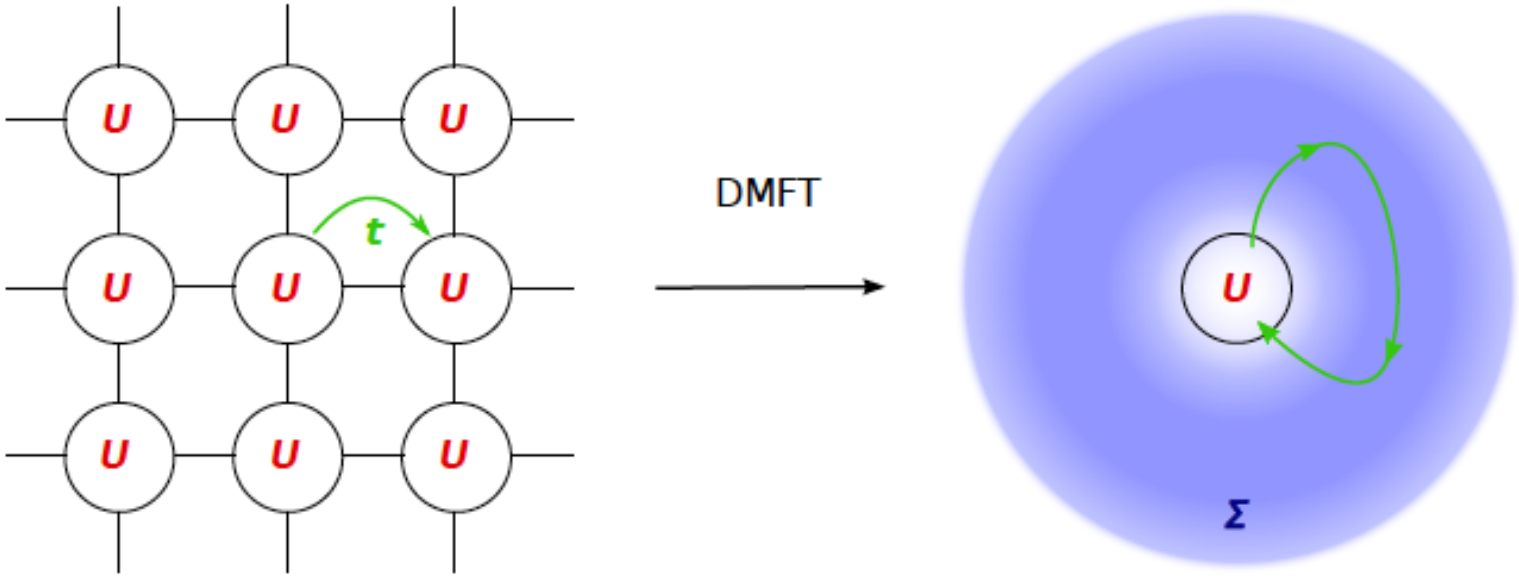


## lattice model

- $e^-$ hop between sites
- local repulsion (screened)

## impurity model

- one interacting site
- non-interacting "bath"

## dynamical mean-field theory

- lattice model ↦ impurity model
- self-energy $\Sigma(\omega)$

Georges et al., RMP 1996,
Kotliar & Vollhardt, Phys. Today 2004

LDA

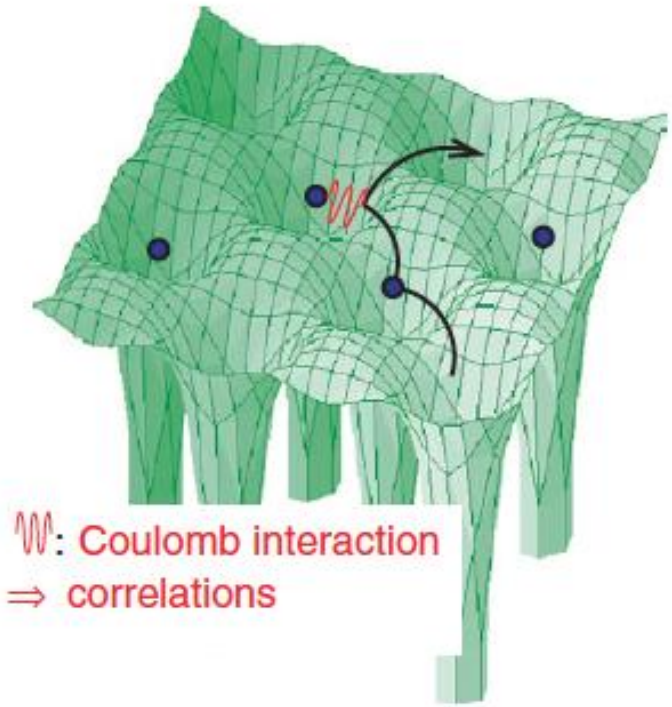


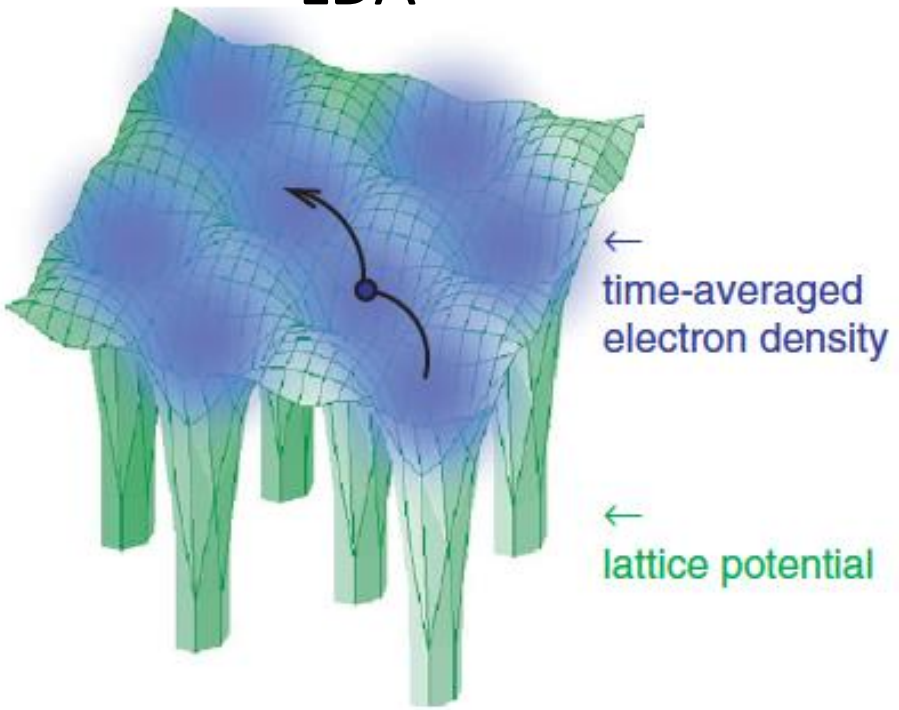


Anderson impurity Hamiltonian

$$H = \sum_{i,j} \epsilon^d_{ij} d^\dagger_i d_j + \frac{1}{2} \sum_{i,j,k,l} U_{ijlk} d^\dagger_i d^\dagger_j d_k d_l$$
$$+ \sum_{ik} (V_{ik} c^\dagger_k d_i + H.c..) + \sum_k \epsilon_k c^\dagger_k c_k$$

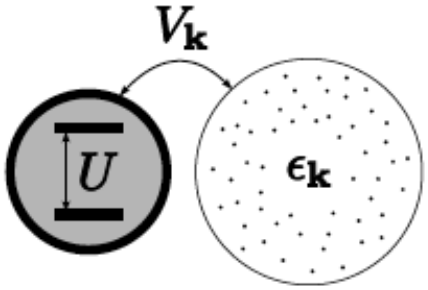

# DMFT: theory vs. experiment

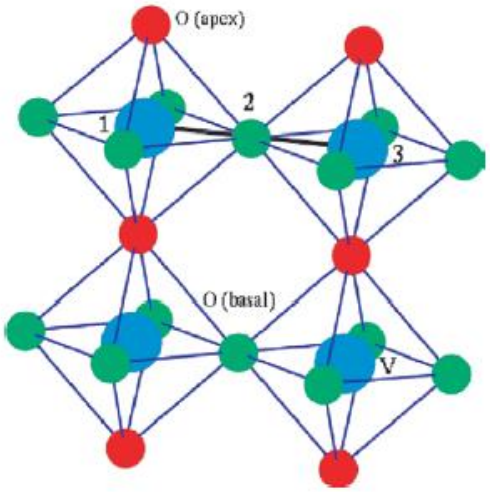


Photoemission

X-ray absorption

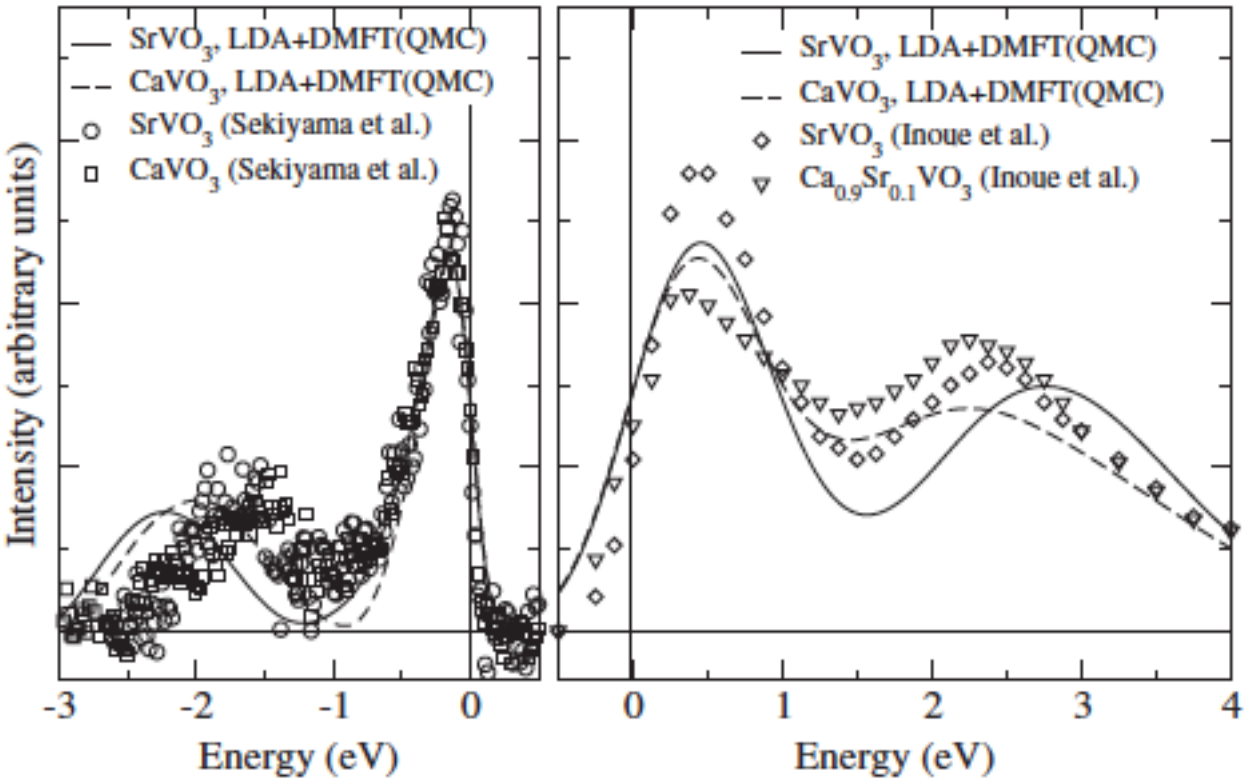


K. Held, Advances in Physics, 56, 829 (2007)

# Multiferroic $BiFeO_3$

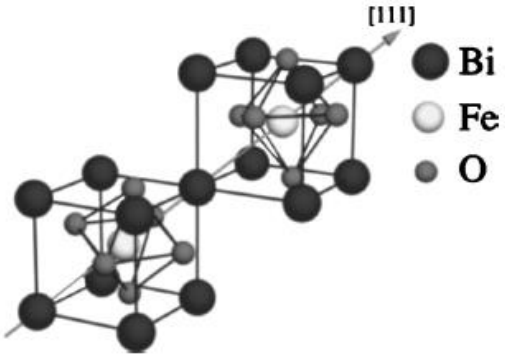


FIG. 1. Structure of $R3c$ $BiFeO_3$. Notice the position of the oxygen octahedra relative to the Bi framework; in the ideal cubic perovskite structure the oxygen ions would occupy the face-centered sites.

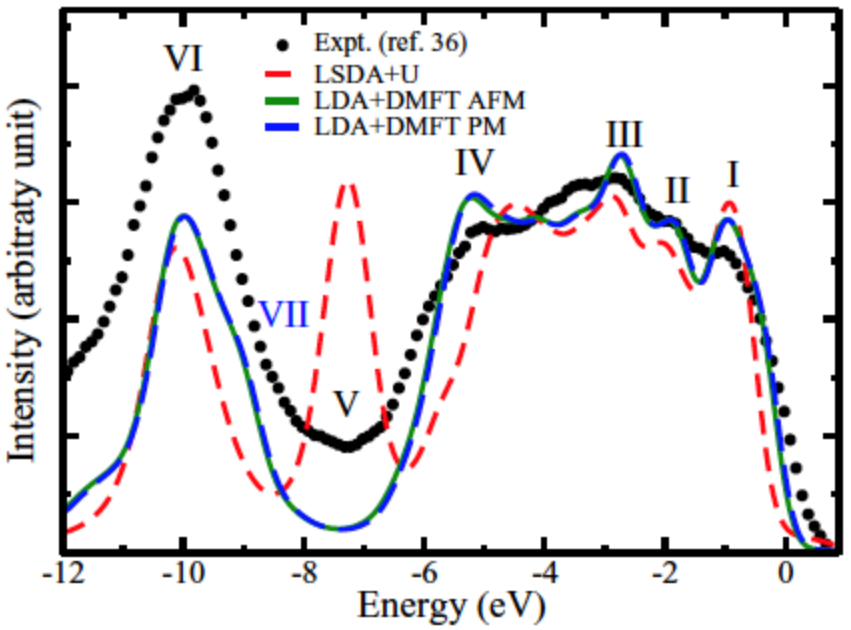


FIG. 5. A comparison between the HAXPES spectra [36] and theoretical spectra of $BiFeO_3$ computed using the LSDA+$U$ and LDA+DMFT methods. The LDA+DMFT spectra are shown for the PM and AFM phases. The theoretical calculations are performed using $U = 6$ eV and $J = 0.9$ eV. The experimental data are shifted to align with the calculated valence-band edge (see text).

Paul et al., PRB (2018)

# Magnetic order

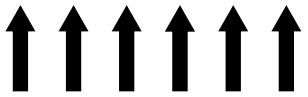

Ferromagnet ($T_C$)

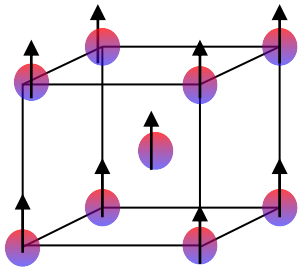

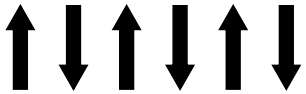

Antiferromagnet ($T_N$)

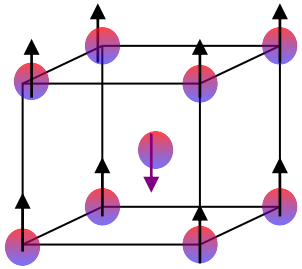

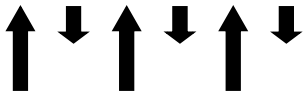

Ferrimagnet

Canted Antiferromagnet

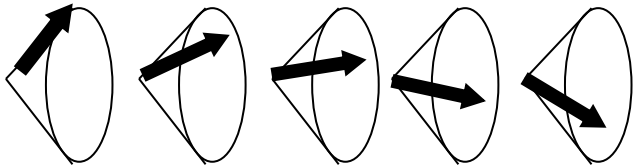

Helical spin spiral

# Spin Hamiltonian

## Isotropic Heisenberg exchange

$$H_{ex}^{bil} = -\sum_{ij} J_{ij}\mathbf{S}_i \cdot \mathbf{S}_j$$

bilinear

$$H_{ex}^{biq} = -\sum_{ij} B_{ij}(\mathbf{S}_i \cdot \mathbf{S}_j)^2$$

biquadratic

## Anisotropic Dzyaloshinskii-Moriya exchange

$$H_{DM} = \sum_{ij} \mathbf{D}_{ij} \cdot (\mathbf{S}_i \times \mathbf{S}_j)$$

Spin-orbit interaction

## Magnetic anisotropy

$$H_{dip} = \sum_{i \neq j} \frac{1}{r_{ij}^3}[\mathbf{M}_i \cdot \mathbf{M}_j - 3(\mathbf{M}_i \cdot \hat{\mathbf{r}}_{ij})(\mathbf{M}_j \cdot \hat{\mathbf{r}}_{ij})]$$

Shape anisotropy
Dipole-dipole interaction

$$H_{SO} = \xi \mathbf{L} \cdot \mathbf{S}$$

Spin-orbit interaction

# Phase transition and critical exponents

Scaling relations

Magnetization $M \sim (T_C - T)^{b}$

Susceptibility $c \sim (T_C - T)^{-g}$

Correlation length $x \sim (T_C - T)^{-n}$

Spin Hamiltonian

$$H = -\sum_{<ij>} J_{ij} S_i . S_j$$

d=1: Ising

d=2: XY

d=3: Heisenberg

# Finite temperature magnetism
## (DFT + Monte Carlo simulations)

**Step 1**

Map DFT to an effective spin model

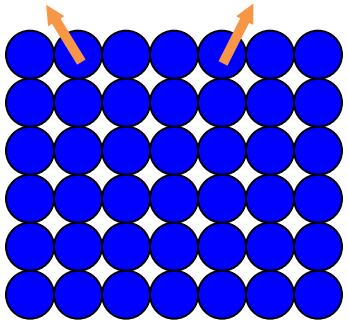

Classical Heisenberg Hamiltonian

$$H = -\sum_{i \neq j} J_{ij} \vec{e}_i . \vec{e}_j$$

$$J_{ij} = \frac{1}{4\pi} \int^{E_F} dE \, \mathrm{Im}\{Tr_L(\Delta_i T_{\uparrow}^{ij} \Delta_j T_{\downarrow}^{ji})\}$$

$T$ : scattering path operator

$$\Delta_i = t_{i\uparrow}^{-1} - t_{i\downarrow}^{-1}$$

$t$ : on-site scattering matrix

$J_{ij}$>0, ferromagnetic

$J_{ij}$<0, antiferromagnetic

# Finite temperature magnetism (contd.)

**Step 2** Monte-Carlo simulations

$$H = -\sum_{i \neq j} J_{ij} \vec{e}_i . \vec{e}_j$$

Metropolis algorithm

Determination of critical temperature :

4th order cumulant crossing method

$$U_L = 1 - \frac{< M^4 >}{3 < M^2 >^2}$$

*M* : magnetization (order parameter)

Also from magnetization/susceptibility/specific heat vs. temperature

# Finite temperature magnetism (contd.)

## Interatomic exchange parameters

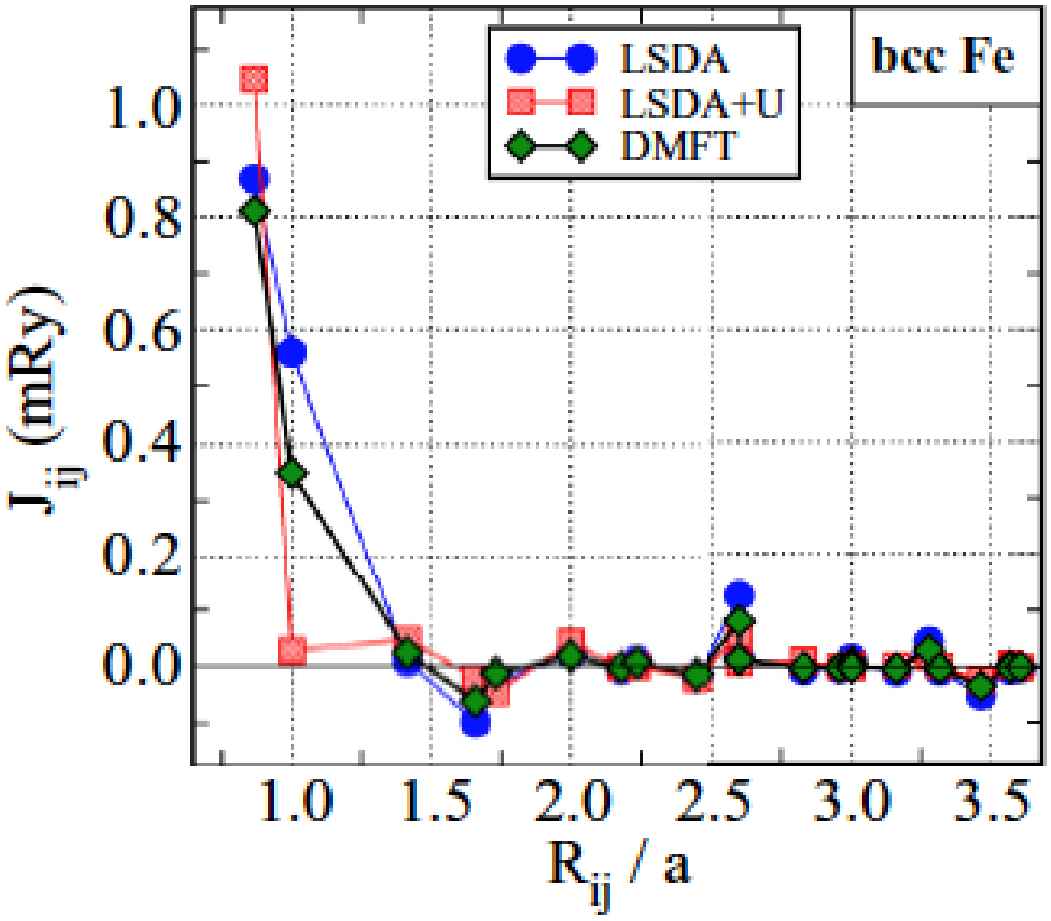


Kvashnin et al., PRB **91**, 125133 (2015)

# Orbital-decomposed exchange parameters

$$J_{ij} = J_{ij}^{E_g - E_g} + J_{ij}^{E_g - T_{2g}} + J_{ij}^{T_{2g} - T_{2g}}$$

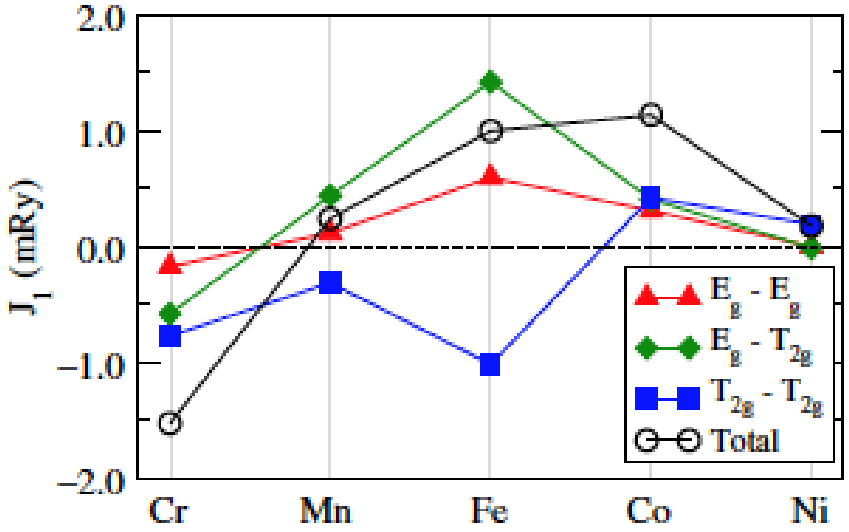


Fe and Mn are different from others

$T_{2g}$-$T_{2g}$ and $E_g$-$E_g$ interactions are opposite in sign

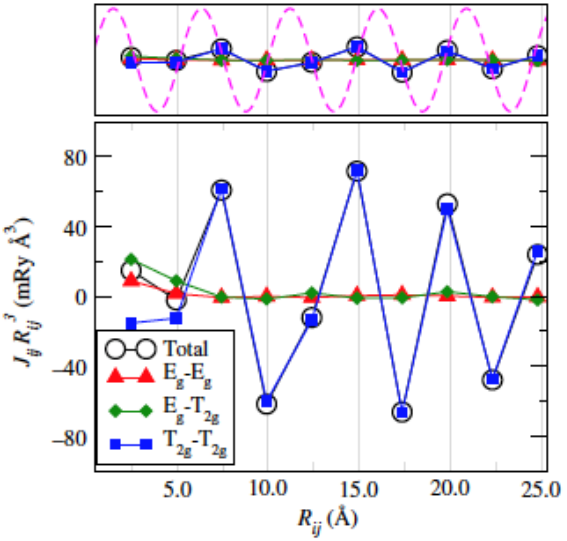


$T_{2g}$-$T_{2g}$ interactions are long ranged.
Also they are the dominant interactions.

PRL **116**, 217202 (2016)

# Analysis of electronic structure

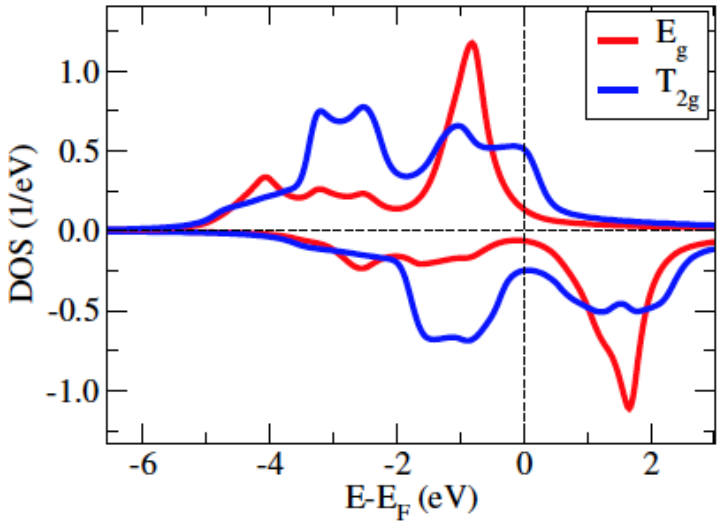


$T_{2g}$ states are dominant at the Fermi level

$T_{2g}$ states contribute to long-range exchange coupling, not $E_g$.

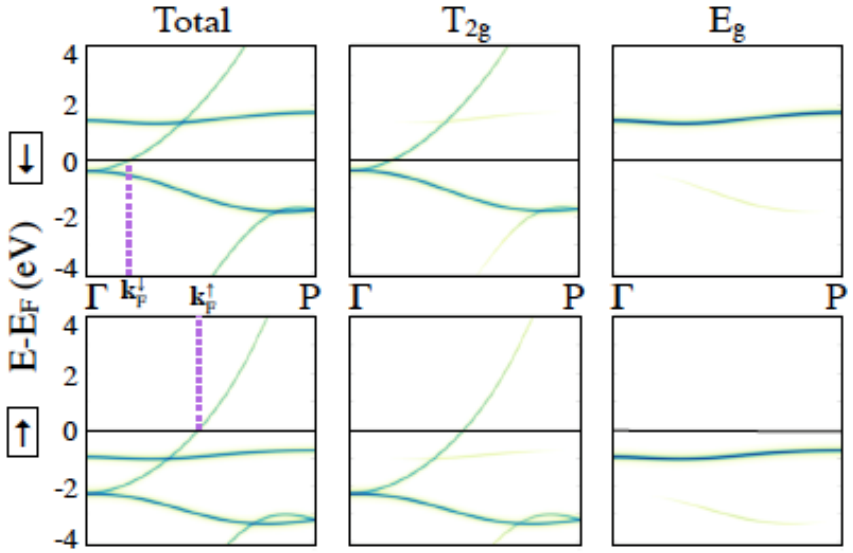


PRL **116**, 217202 (2016)

# Finite temperature magnetism (contd.)

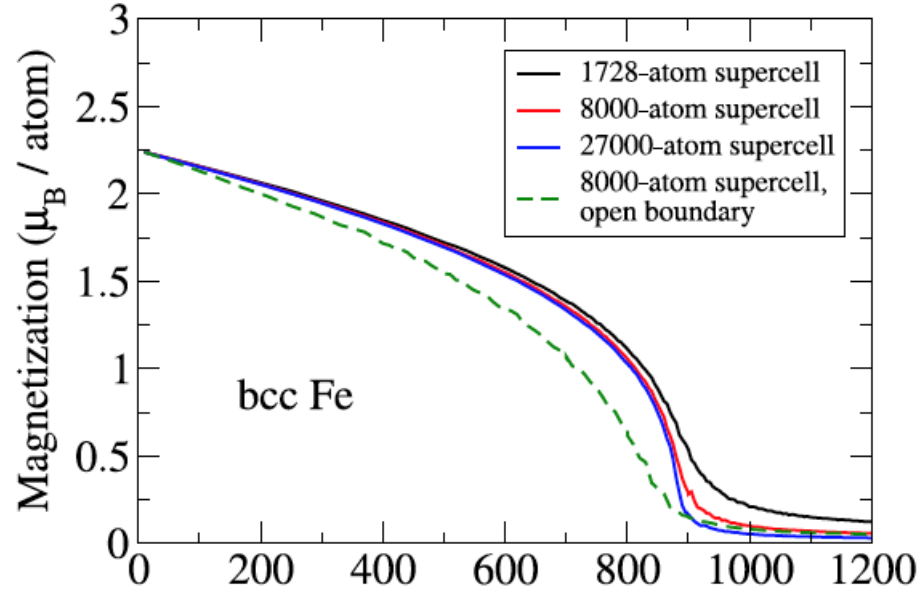


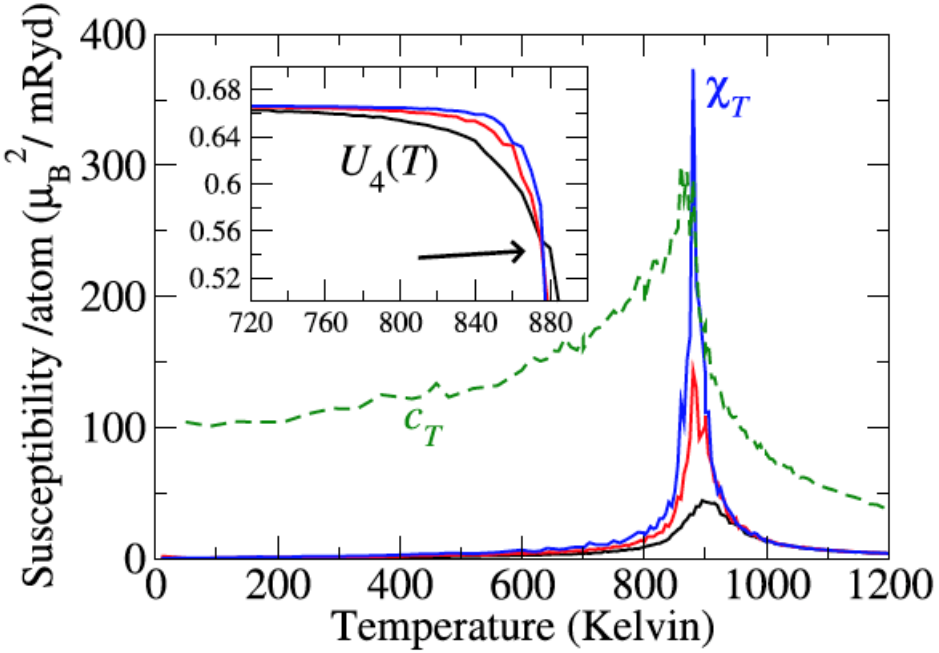


BCC Fe

Experimental $T_C$: 1043 K

Theoretical $T_C$: ~900 K

Mavropoulos, IFF Spring School ('14)

# Quadruple perovskite $PbCu_3Fe_2Re_2O_{12}$

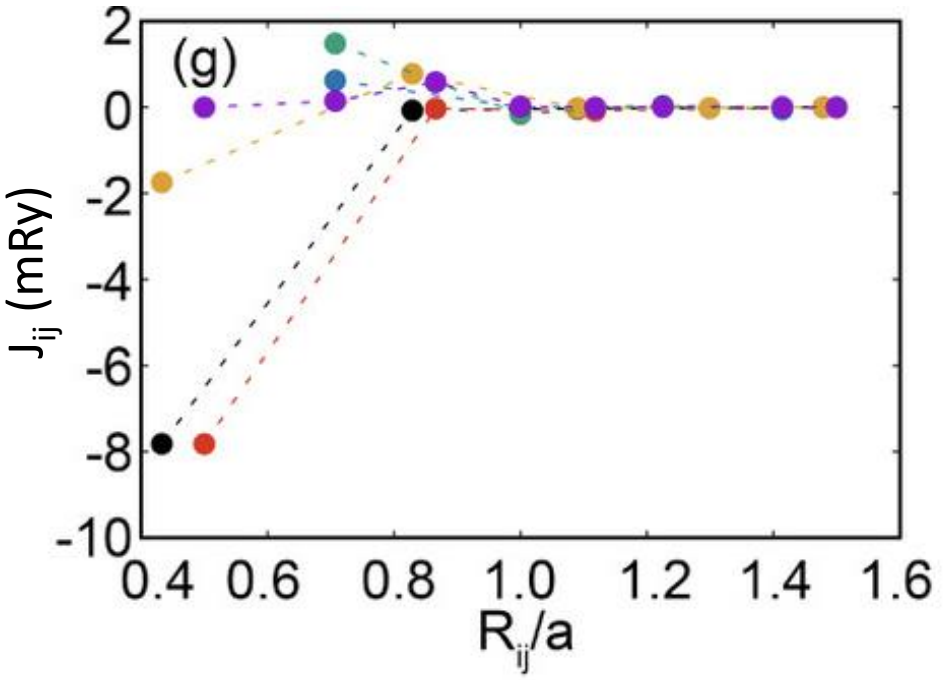


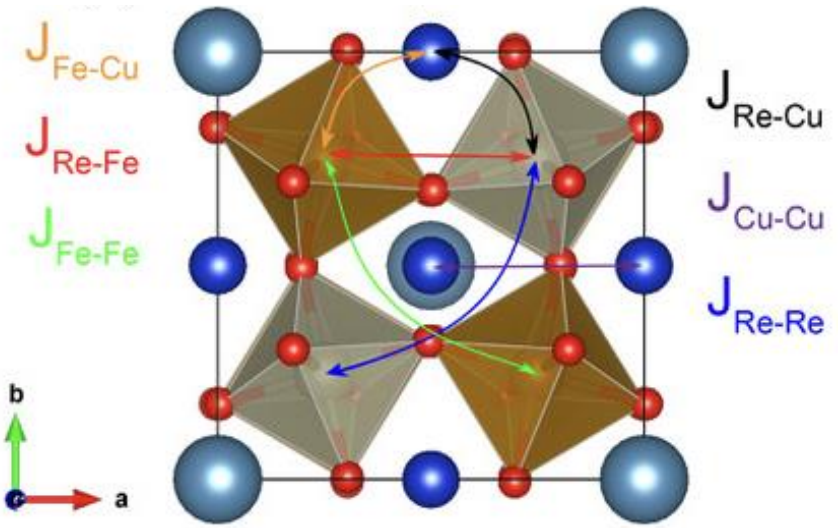


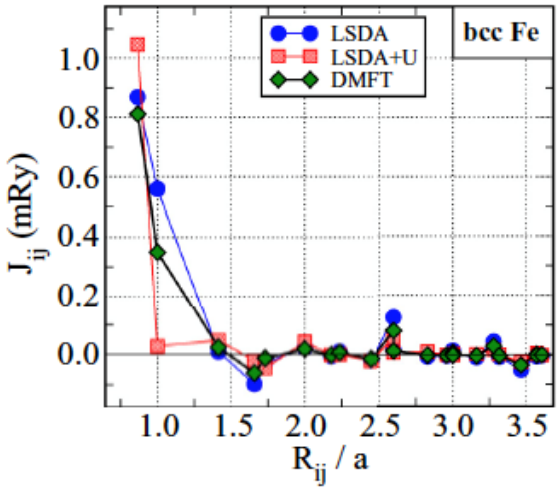

# Spin-orbit interaction in solids

Magnetic anisotropy:
(i) magnetocrystalline anisotropy (ii) shape anisotropy

Magnetocrystalline anisotropy energy (MCA):
Energy required to rotate the magnetization from the 'easy' direction to the 'hard' direction.

$$\Delta E_{so} = \langle H_{so} \rangle_{hard} - \langle H_{so} \rangle_{easy} = \zeta [\langle \mathbf{L} \cdot \mathbf{S} \rangle_{hard} - \langle \mathbf{L} \cdot \mathbf{S} \rangle_{easy}] > 0$$

MCA ~ $10^{-5}$ eV/atom

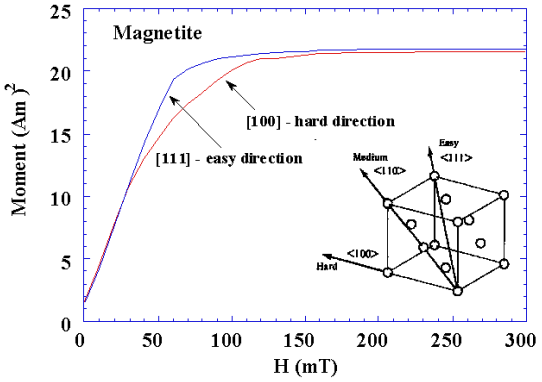


Bruno model

Magnetic anisotropy energy is directly related to the anisotropy in orbital moments

$$\Delta E_{so} = \zeta [\langle \mathbf{L} \cdot \mathbf{S} \rangle_{hard} - \langle \mathbf{L} \cdot \mathbf{S} \rangle_{easy}] = \frac{\zeta}{4\mu_B} (m_o^{easy} - m_o^{hard}) > 0$$

## 2nd order perturbation theory

$$\Delta E_{so} = E_z - E_x \approx \zeta^2 \sum_{u,o,\sigma,\sigma'} [\frac{|\langle u^\sigma|\mathbf{L}_z|o^{\sigma'}\rangle|^2 - |\langle u^\sigma|\mathbf{L}_x|o^{\sigma'}\rangle|^2}{\epsilon_u^\sigma - \epsilon_o^{\sigma'}}]$$

o,u: occupied, unoccupied states.
ε's are the energy eigenvalues

## Shape anisotropy

(arising from magnetic dipole-dipole interaction)

$$E_{dip} = \frac{\mu_0}{8\pi} \sum_{i \neq j} \frac{1}{r_{ij}^3} [\mathbf{m}_i \cdot \mathbf{m}_j - 3\frac{(\mathbf{r}_{ij} \cdot \mathbf{m}_i)(\mathbf{r}_{ij} \cdot \mathbf{m}_i)}{r_{ij}^2}]$$

If the magnetic moments are parallel,

$$E_{dip} = \frac{\mu_0}{8\pi} \sum_{i \neq j} \frac{m_i m_j}{r_{ij}^3} (1 - 3cos^2\theta_{ij})$$

$\theta_{ij}$ is the angle between the direction of the magnetic moment and the vector connecting *i* and *j*.

# Comparison between theory & experiments

Cubic crystals, bcc & fcc: $\Delta E=E(001)-E(111)$
Hcp Co: $\Delta E=E(0001)-E(10\text{-}10)$

Magnetocrystalline anisotropy ($\Delta E$ in $\mu$eV/atom)

| | **Fe (bcc)** | **Co (hcp)** | **Co (fcc)** | **Ni (fcc)** |
|---|---|---|---|---|
| Exp. | -1.34 | -65 | 1.66 | 2.7 |
| Theory | -2.6/-1.8 | -110 | 2.4/2.2 | 1.0/-0.5 |

# The world of 2D materials

2004: First synthesis of graphene
2010: Nobel prize to Geim & Novoselov

van der Waals heterostructures

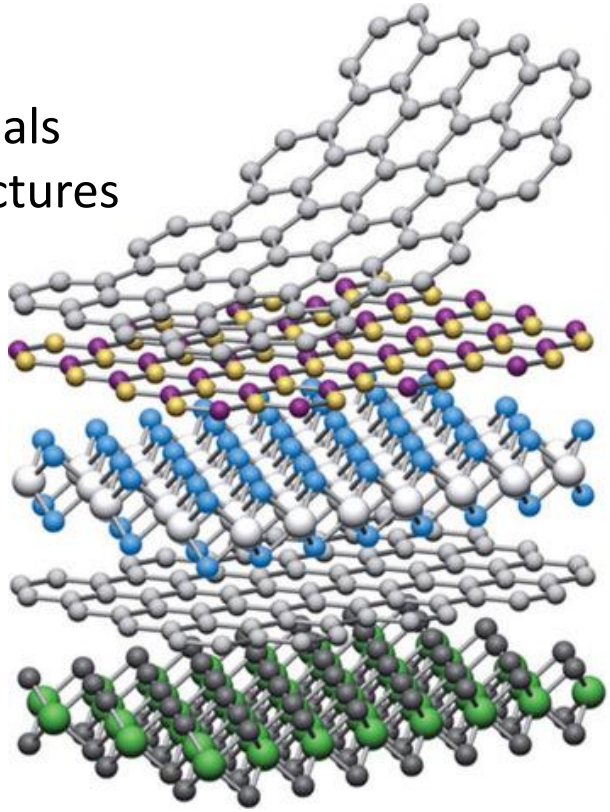

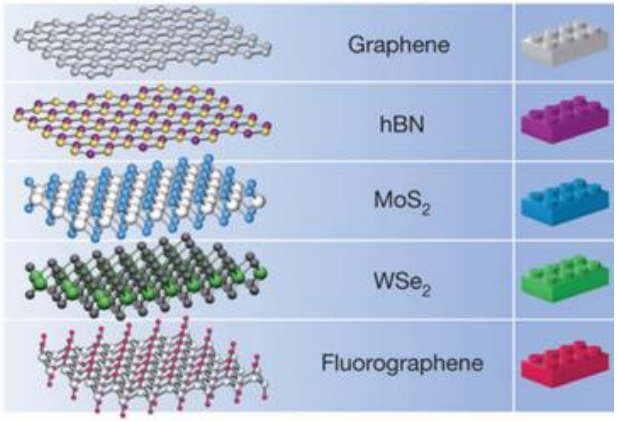


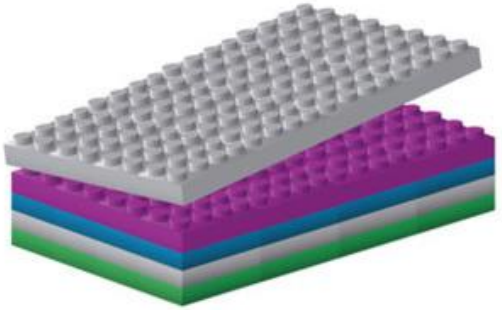

Lego building

*Nature* ***499***, 419 (2013)

**New addition:**
**2D magnetism (magnetic long-range order in atomically thin materials)**

# 2D magnets

**Mermin-Wagner theorem**: long-range magnetic order is prohibited in the 2D isotropic-Heisenberg model with short-ranged interactions at a finite temperature

**Magnetic anisotropy** removes this restriction

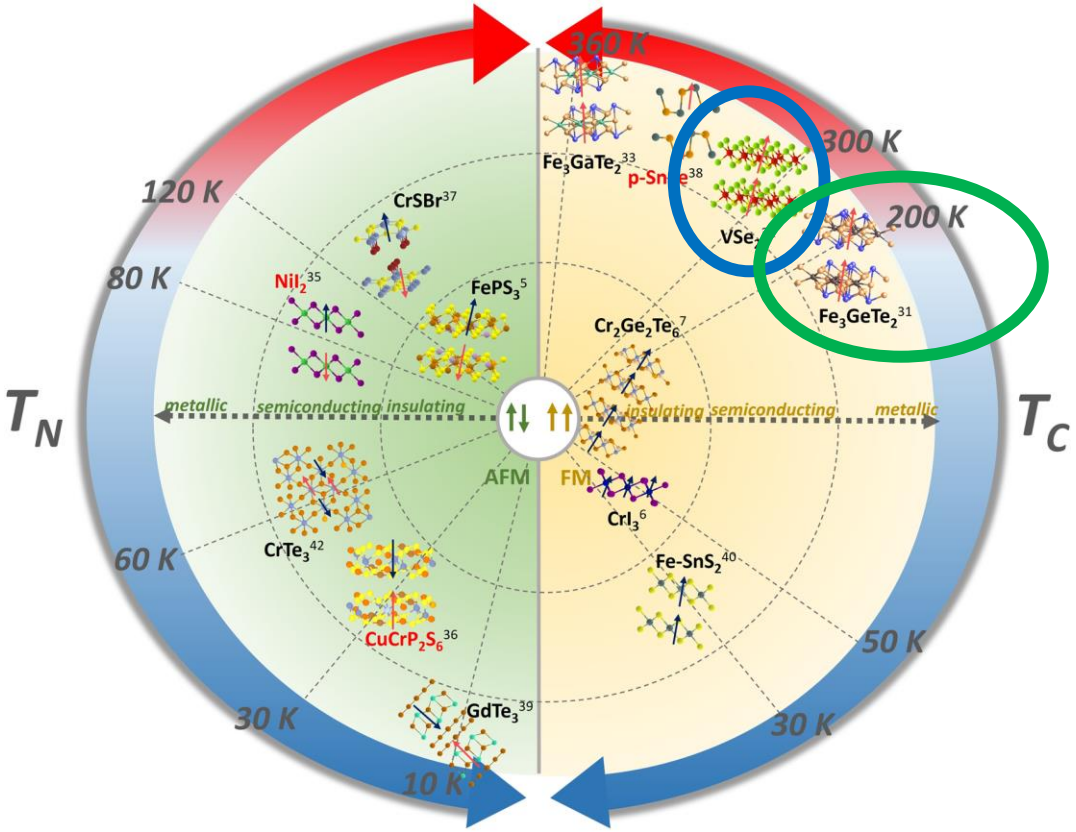


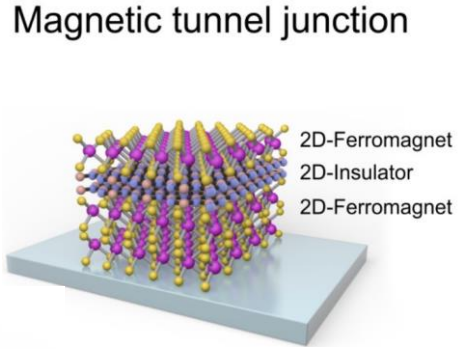


npj Spintronics 2, 6 (2024)

Nat. Nanotech. 16, 856 (2021)

UPPSALA UNIVERSITET

# Interfacial engineering of 2D magnetism

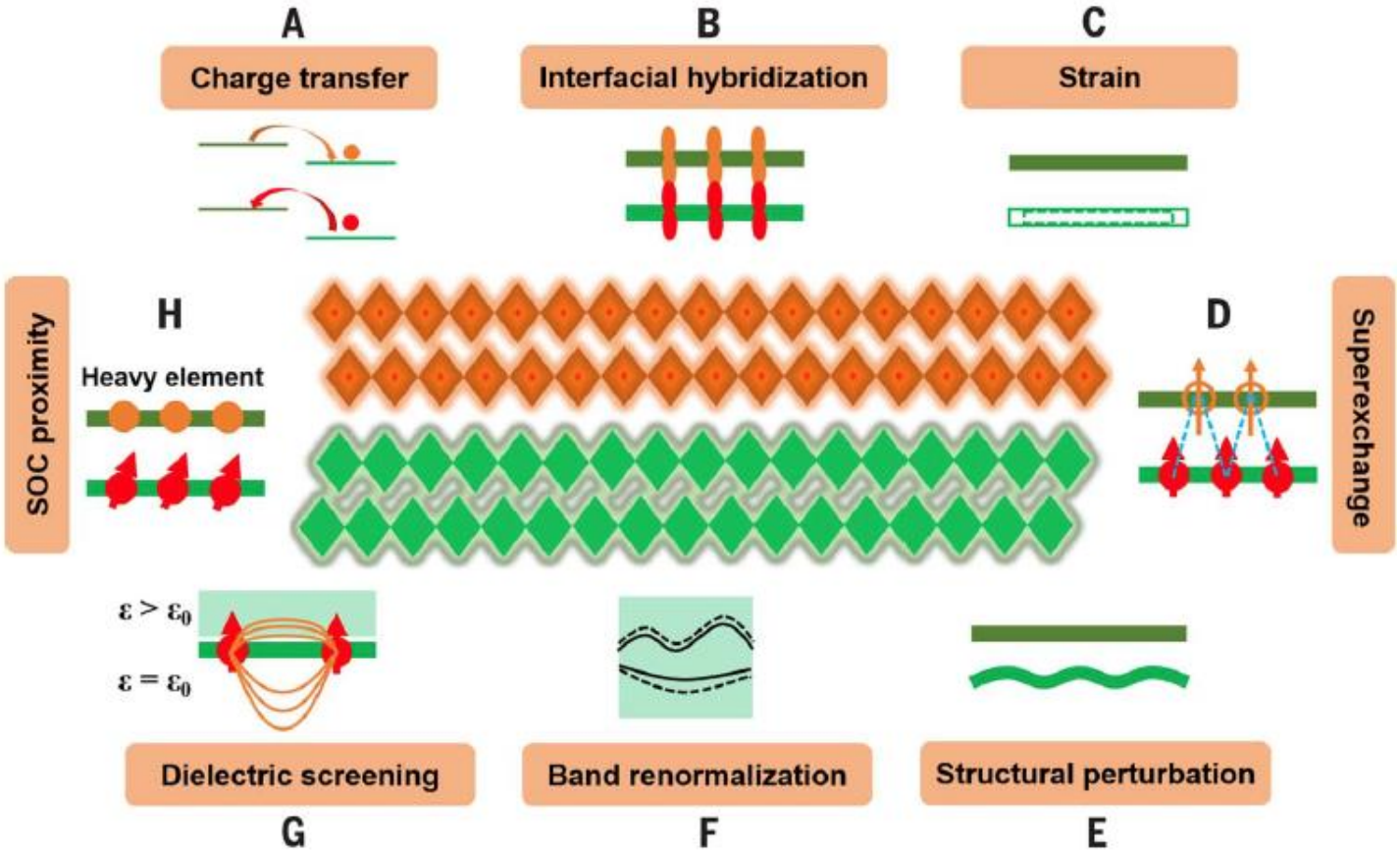


*Nature* **546**, 270 (2017)
Science **363**, eaav4450 (2019)

UPPSALA UNIVERSITET

# 2D vdW magnet $Fe_3GeTe_2$

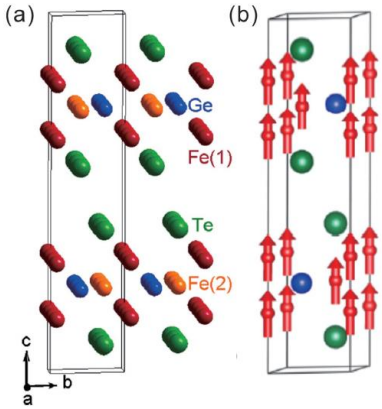


Metallic ferromagnet
Strong out-of-plane anisotropy
$T_C$=207K (bulk)
$T_C$=130K (ML)

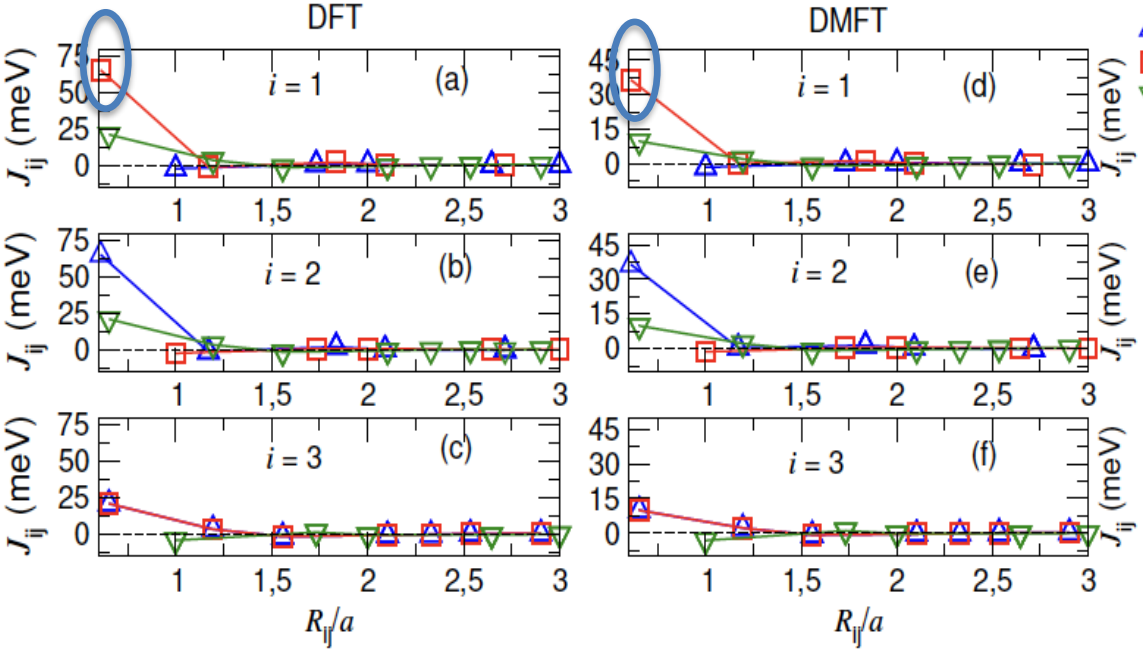


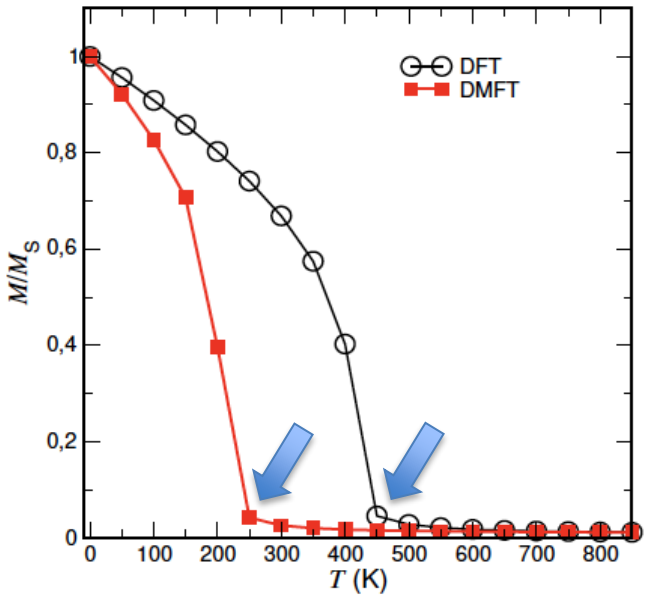


Strong reduction of exchange parameter and $T_C$ (better comparison with experiment)

Ghosh, Ershadrad, Borisov & Sanyal, npj. Comp. Mater. **9**, 86 (2023)

# Bilayer $Fe_3GeTe_2$-O/$HfTe_2$

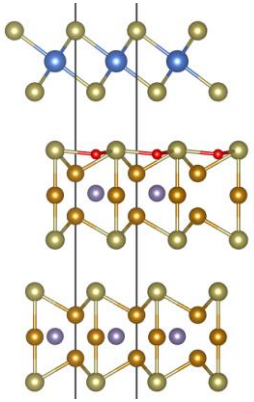


## Micromagnetic parameters

| Structure | A (meV. Å$^2$) | D (meV. Å) | K (meV/f.u.) | M ($\mu_B$/f.u.) |
|---|---|---|---|---|
| Bilayer $Fe_3GeTe_2$-O | 234 | 8.2 | 1.4 | 6.6 |
| Bilayer $Fe_3GeTe_2$-O/$HfTe_2$ | 194 | 18.4 | 1.4 | 6.5 |

$$D_{\alpha\beta} = \sum_{j \neq i} D_{ij}^{\alpha} R_{ij}^{\beta} \, e^{-\mu R_{ij}}$$

$$A = \frac{1}{2} \sum_{j \neq i} J_{ij} R_{ij}^{2} \, e^{-\mu R_{ij}}$$

## Formation of skyrmions

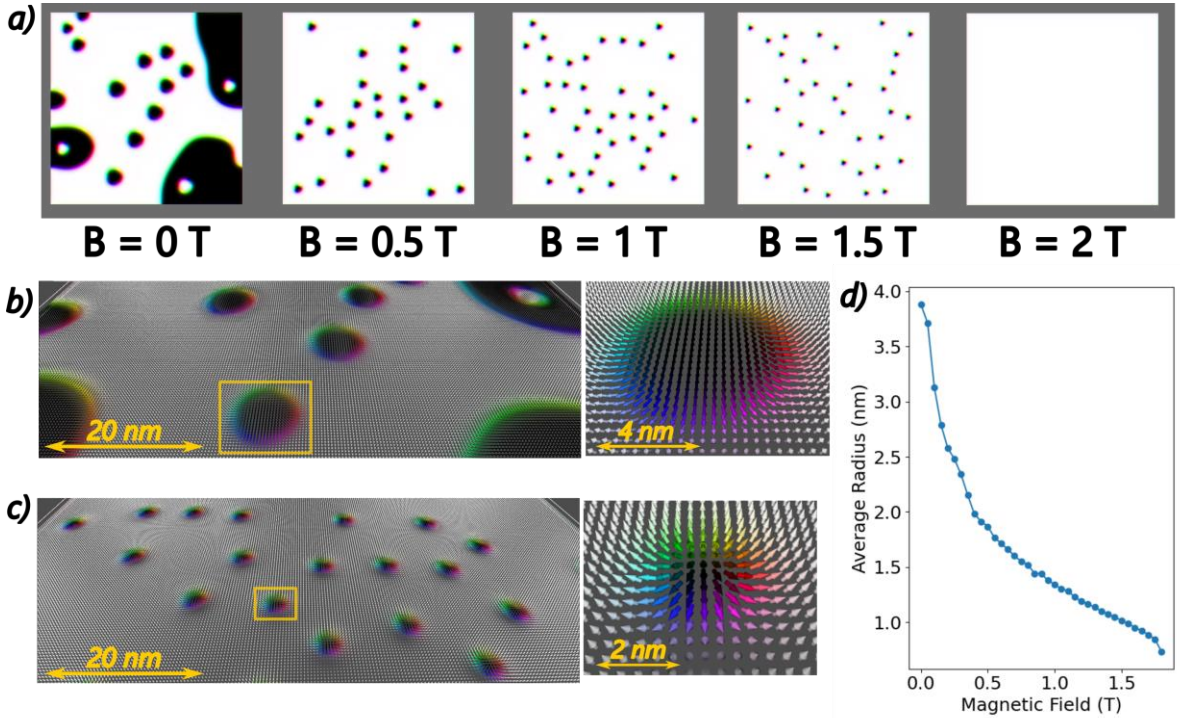


Machacova, Ershadrad, Sanyal (unpublished)

# Laser induced ultrafast magnetization switching

Ultrafast demagnetization of Ni

Pump-probe (60 fs laser pulse)

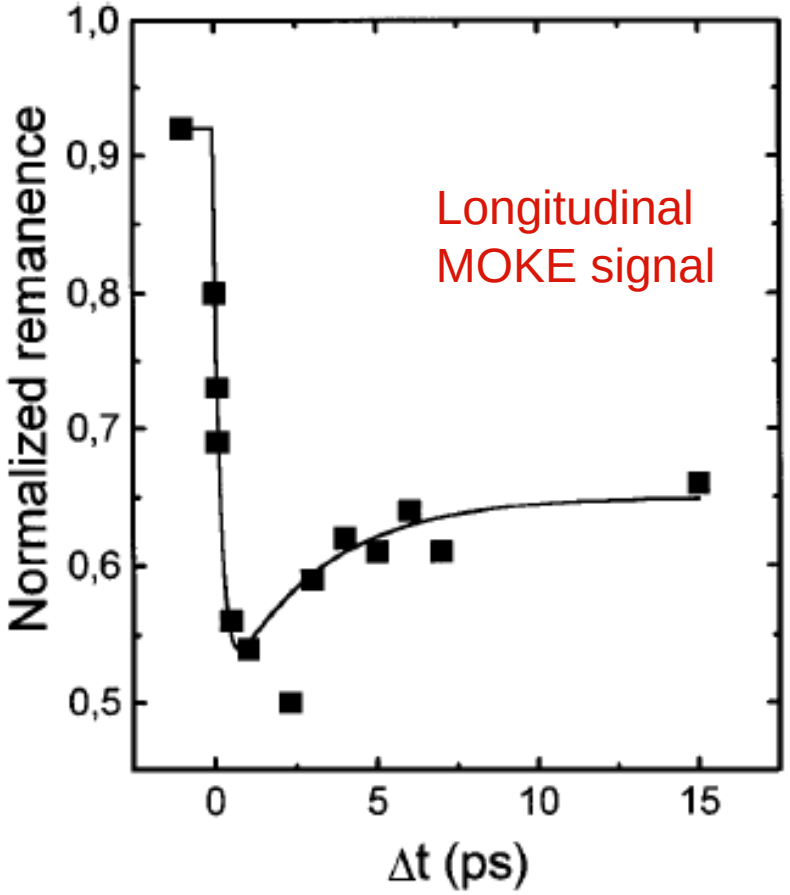


Beaurepaire et al., PRL **76**, 4250 (1996)

Coupled subsystems

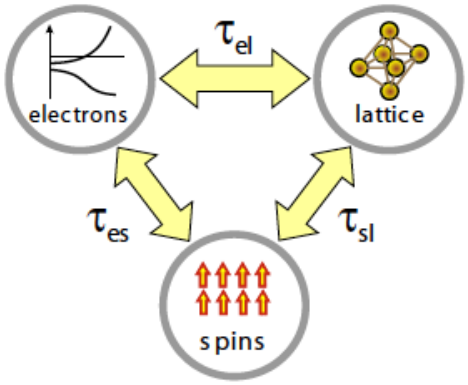


Rep. Prog. Phys. **76**, 026501 (2013)

Phenomenological 3 temperature model

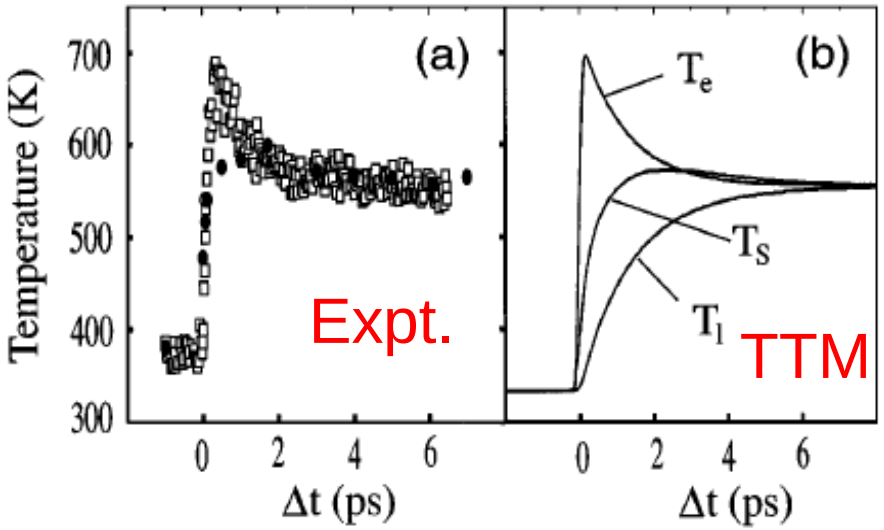

# Atomistic spin dynamics simulations

Landau-Lifshitz-Gilbert equation of motion

$$\frac{d\mathbf{m}_i}{dt} = -\gamma \mathbf{m}_i \times [\mathbf{B}_i + \mathbf{b}_i(t)] - \gamma \frac{\alpha}{m} \mathbf{m}_i \times (\mathbf{m}_i \times [\mathbf{B}_i + \mathbf{b}_i(t)])$$

precession damping

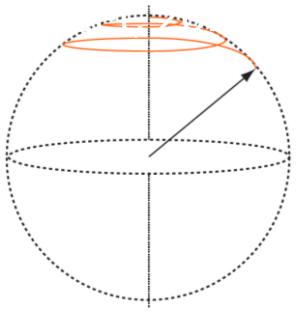

Effective field $\mathbf{B}_i = -\frac{\partial H}{\partial \mathbf{m}_i}$

$\mathbf{b}_i(t)$: Stochastic magnetic field

$\alpha$ : damping parameter

$\gamma$ : electron gyromagnetic ratio

Exchange (classical Heisenberg)

$$H_{ex} = -\frac{1}{2} \sum_{i \neq j} J_{ij} \mathbf{m}_i \times \mathbf{m}_j$$

Dzyaloshinskii-Moriya (spin-orbit coupling)

$$H_{DM} = \sum_{ij} \mathbf{D}_{ij} \times (\mathbf{S}_i \times \mathbf{S}_j)$$

Skubic *et al.*, J. Phys: Condens. Matt. **20**, 315203 (2008)

Atomistic spin dynamics webpage: http://www.physics.uu.se/cmt/asd

Home grown code: UppASD

# Ultrafast magnetization dynamics (ab initio theory + spin dynamics)

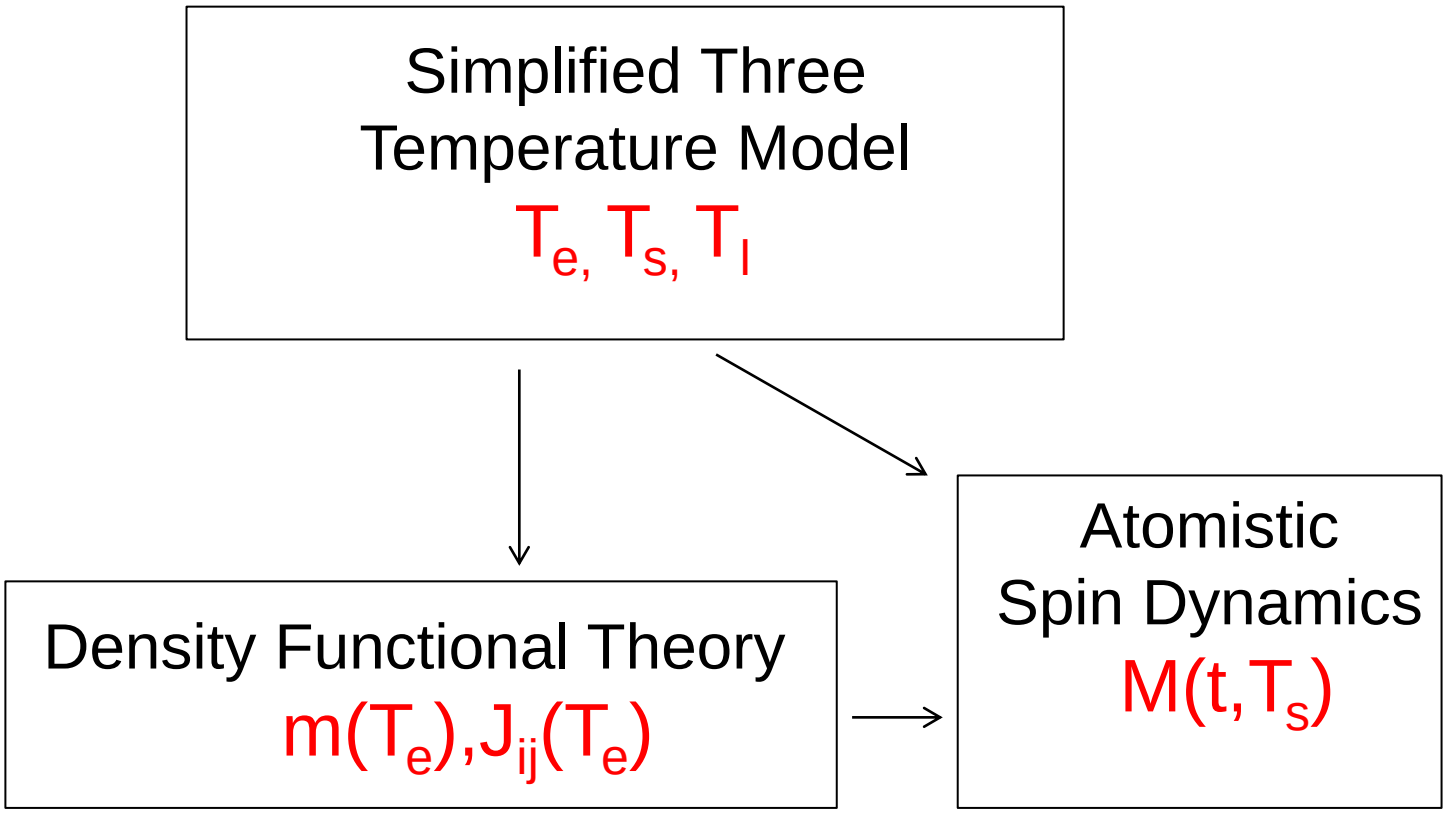

# Magnetization switching in amorphous **ferrimagnetic** GdFe alloys

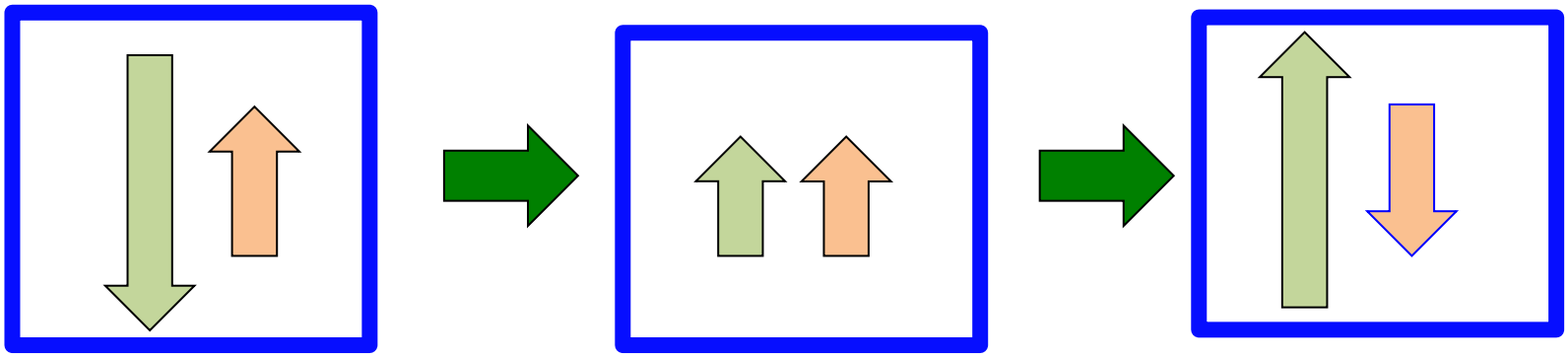

-1 ps 0.5 ps > 2 ps

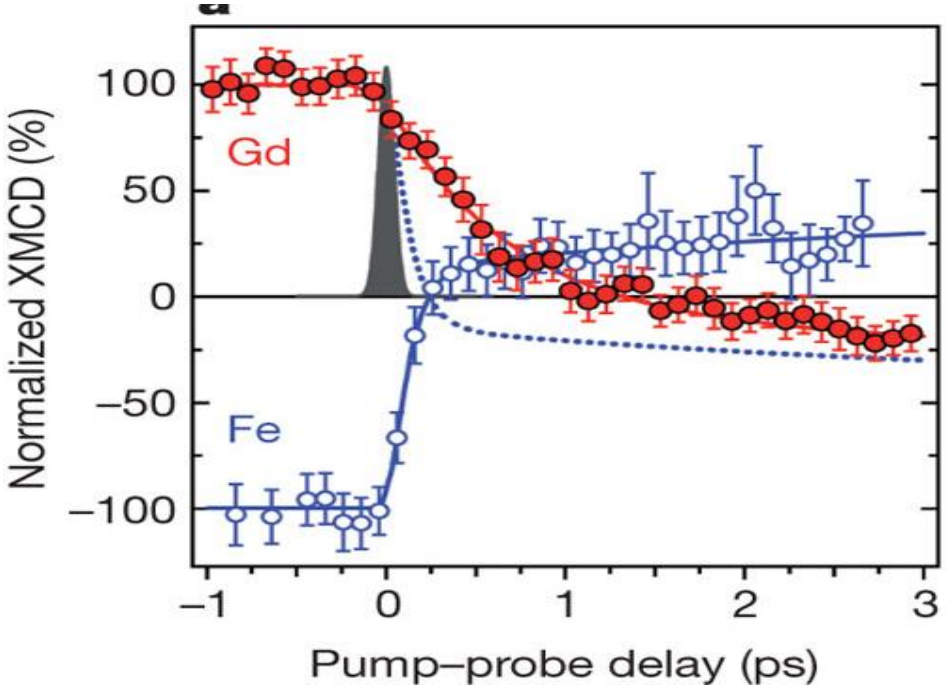


Radu et al., Nature **472**, 205 (2011)

# Local demagnetization & inhomogeneities

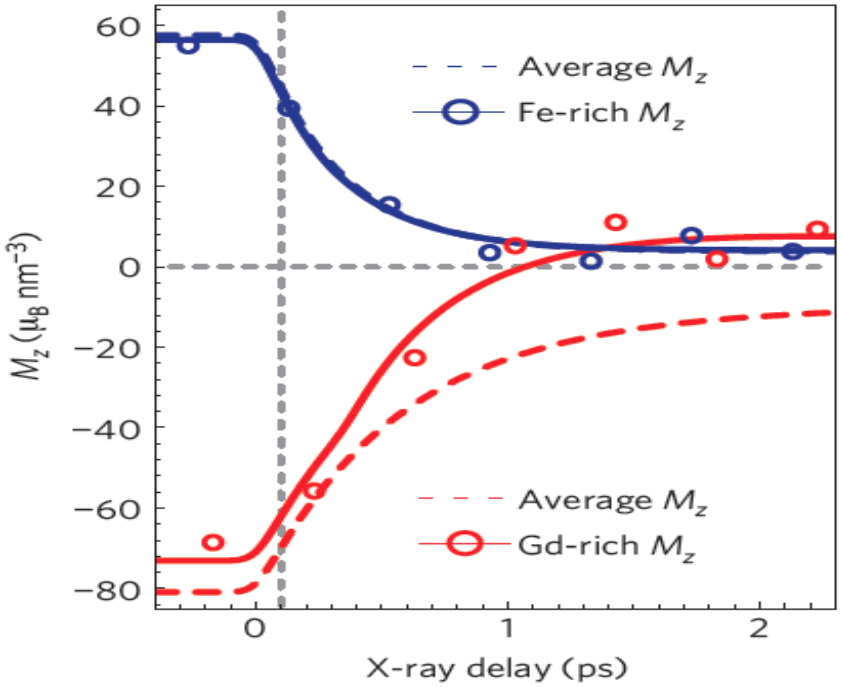


Different switching behavior for average concentration and Gd/Fe rich conditions

Graves et al.,
Nat. Mater. **12**, 293 (2013)

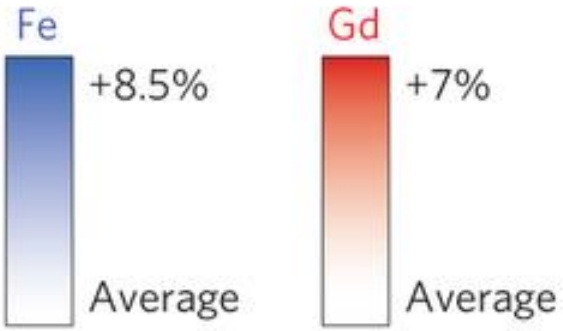


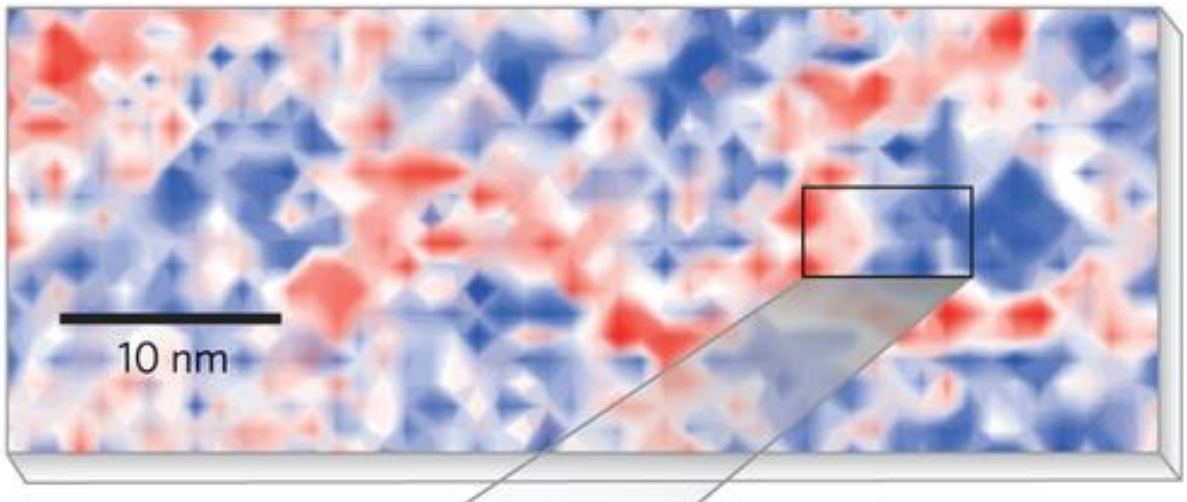

# Switching times (inhomogeneous vs. average)

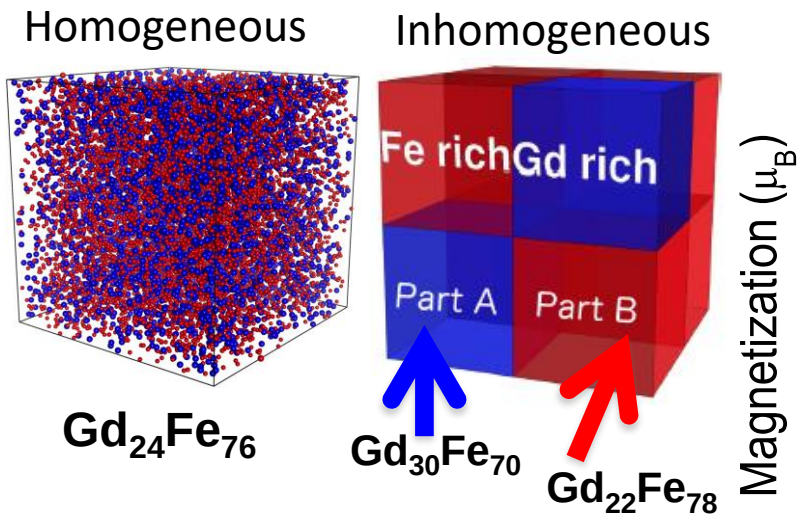


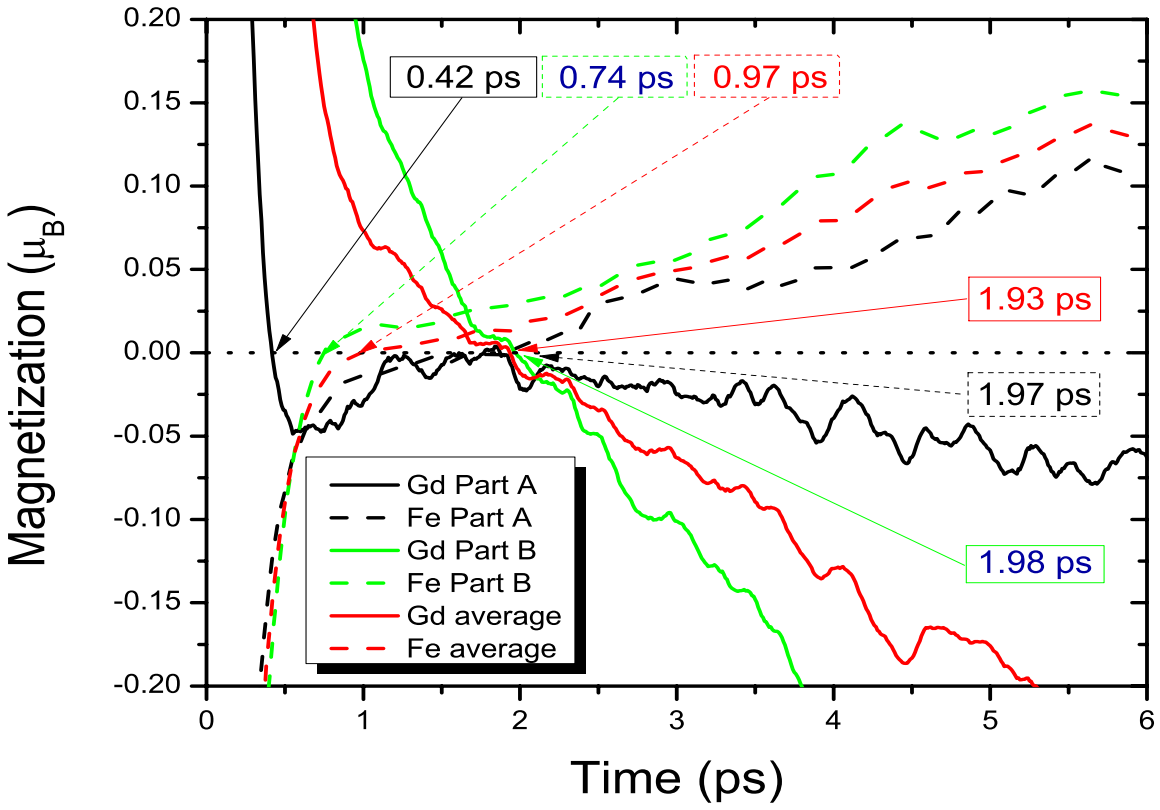


- DFT calculations indicate canting of Gd moments in Gd-rich regions.
- Inclusion of next nearest neighbor $J_2$ and hence non-collinear magnetism yields faster Gd switching than Fe

NN $J_1$=0.25mRy

NNN $J_2$=0.0 -0.4 mRy

Correctly reproduces the contrasting experimental observations

Chimata et al., Phys. Rev. B **92,** 094411 (2015)

# Summary

- Short introduction to (s)DFT
- Spin dipole moments
- Electron correlation (DFT+U & DMFT)
- Magnetic exchange interactions
- Magnetic anisotropy
- 2D magnets
- Atomistic spin dynamics simulations